Table 2. Variation among individuals determined with qPCR*

Group	Relative expression (Exp/Cont, Mean ± SD)				
	Gapdh	*c-Jun*	*Ccng1*	*Hsp27*	*Rad52*
Saline 4 h	1.00 ± 0.14	1.00 ± 0.26	1.00 ± 0.18	1.00 ± 0.07	1.00 ± 0.14
DEN 4 h	0.92 ± 0.14	13.71 ± 2.11	6.50 ± 0.86	2.47 ± 0.47	1.56 ± 0.23
Saline 28 d	1.00 ± 0.07	1.00 ± 0.24	1.00 ± 0.16	1.00 ± 0.12	1.00 ± 0.12
DEN 28 d	1.03 ± 0.09	1.15 ± 0.26	1.57 ± 0.21	0.83 ± 0.07	0.97 ± 0.06

*Experiment III, livers from 5 mice each of experimental groups (4 h and 28 days) and control group were used. Mean of control group is presented as 1.00.

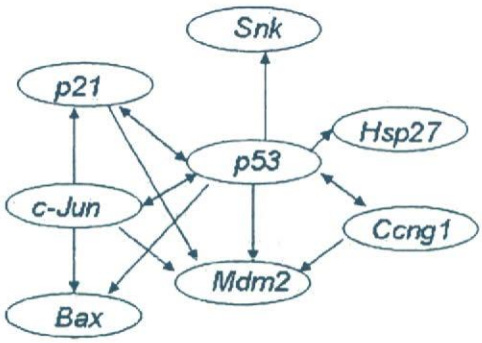

Fig. 6. Suggested gene network of seven *p53* target genes analyzed using Ingenuity Pathways Analysis.

material were desirable.

Recent reports have described changes in gene expression in DEN-induced mouse liver tumors (22–24) and DEN-treated rat liver (25) with different DNA microarrays containing different genes, but no studies have focused on the DNA damaging time of 4 h nor the mutation fixing time of 28 days; thus, different gene expressions were detected. As well, there are no reports which compare changes in gene expression in mouse liver for DEN and DPN exposures. The present study showed that DEN and DPN induced very similar changes in gene expression in mouse liver at 4 h and 28 days after their administration, suggesting a similar response mechanism. Gene expression changes with PB (25–27) and EtOH (28) were previously studied in mouse or rat liver at different time points with different DNA microarrays containing different genes, resulting in different gene expressions being detected.

In the present DNA microarray we mainly selected genes that have been linked with the action of genotoxic carcinogens. As a result we could find characteristic gene expression increases for DEN and DPN, but we could not find genes that were specifically responsive to the non-genotoxic carcinogen PB or to the non-carcinogenic toxin EtOH. Decreased-expression genes were observed among the 268 genes in the present results (not shown). However, characteristically decreased genes were not found for DEN, DPN, PB or EtOH in the present 268 gene-list.

In the first step of characterizing our microarray system, we examined 20mer, 30mer and 40–47mer oligonucleotides as probes (data not shown) and concluded that 40–47mer oligonucleotides showed sufficient strength of fluorescence. In an early trial, we prepared cDNA microarray with PCR products of 400 bp length. However these cDNA microarrays were less sensitive than the present oligonucleotide microarray (data not shown).

In conclusion, we have used DNA microarray and qPCR to show (1) that in comparison to PB and EtOH, the genotoxic carcinogens DEN and DPN induced differential gene expression in *p53* target genes in mouse liver 4 h after chemical administration (a time when DNA damage is induced by *N*-nitroso carcinogens), and (2) that these acute responses remained only partially in liver 28 days after administration, a time when little DNA damage remains but mutations are observed. We will continue further studies to add other useful genes to our DNA microarray, including high throughput DNA microarray studies in mouse liver and preparation of in-house oligonucleotide microarray for characterizing mutagenic and carcinogenic compounds; these data will be applied to the study of chemical risk assessment.

Acknowledgements: This work was partly supported by Special Coordination Funds for Promoting Science and Technology (C. Furihata and H. Tashiro) and by KAKENHI (18310047) (C. Furihata, T. Watanabe and T. Suzuki), The Ministry of Education, Culture, Sports, Science and Technology, Japan. We thank Drs. Yoshifumi Uno (Mitsubishi Pharma Co.), Yasuhito Yamamoto (Lion Co.), Yuko Saito (NIKKEN CHEMICALS CO., LTD), Kohji Yamakage (Hatano Research Institute, Food and Drug Safety Center) and Akihiro Wakata (Yamanouchi Pharmaceutical Co., Ltd.) (members of JEMS/MMS/Toxicogenomics collaborative study) for stimulating discussions.

References

1 Aardema MJ, MacGregor JT. Toxicology and genetic

toxicology in the new era of "toxicogenomics": impact of "-omics" technologies. Mutat Res. 2002; 499: 13-25.
2 Dupuy A, Simon RM. Critical review of published microarray studies for cancer outcome and guideline on statistical analysis and reporting. J Natl Cancer Inst. 2007; 99: 147-57.
3 Ulger C, Toruner GA, Alkan M, Mohammed M, Damani S, Kang J, Galante A, Aviv H, Soteropoulos P, Tolias PP, Schwalb MN, Dermody JJ. Comprehensive genome-wide comparison of DNA and RNA level scan using microarray technology for identification of candidate cancer-related genes in the HL-60 cell line. Cancer Genet Cytogenet. 2003; 147: 28-35.
4 Mecham BH, Klus GT, Strovel J, Augustus M, Byrne D, Bozso P, Wetmore GZ, Mariani TJ, Kohane IS, Szallasi S. Sequence-matched probes produce increased cross-platform consistency and more reproducible biological results in microarray-based gene expression measurements. Nucleic Acids Res. 2004; 32: e74.
5 Shippy R, Sendera TJ, Lockner R, Palaniappan C, Kaysser-Kranich T, Watts G, Alsobrook J. Performance evaluation of commercial short-oligonucleotide microarrays and the impact of noise in making cross-platform correlations. BMC Genomics. 2004; 5: 61.
6 Provenzano M, Mocellin S. Complementary techniques: validation of gene expression data by quantitative real time PCR. Adv Exp Med Biol. 2007; 593: 66-73.
7 Mientjes EJ, Luiten-Schuite A, van der Wolf E, Borsboom Y, Bergmans A, Berends F, Lohman PH, Baan RA, van Delft JH. DNA adducts, mutant frequencies, and mutation spectra in various organs of lambda lacZ mice exposed to ethylating agents. Environ Mol Mutagen. 1998; 31: 18-31.
8 Madle S, Dean SW, Andrae U, Brambilla G, Burlinson B, Doolittle DJ, Furihata C, Hertner T, McQueen CA, Mori H. Recommendations for the performance of UDS tests *in vitro* and *in vivo*. Mutat Res. 1994; 312: 263-85.
9 Sasaki YF, Sekihashi K, Izumiyama F, Nishidate E, Saga A, Ishida K, Tsuda S. The comet assay with multiple mouse organs: comparison of comet assay results and carcinogenicity with 208 chemicals selected from the IARC monographs and U.S. NTP Carcinogenicity Database. Crit Rev Toxicol. 2000; 30: 629-799.
10 Suzuki T, Hayashi M, Sofuni T. Initial experiences and future directions for transgenic mouse mutation assays. Mutat Res. 1994; 307: 489-94.
11 Suzuki T, Itoh S, Nakajima M, Hachiya N, Hara T. Target organ and time-course in the mutagenicity of five carcinogens in MutaMouse: a summary report of the second collaborative study of the transgenic mouse mutation assay by JEMS/MMS. Mutat Res. 1999; 444: 259-68.
12 Furihata C, Oka M, Yamamoto M, Ito T, Miki K, Tatematsu M, Sakaki Y, Reske K. Differentially expressed MHC class II-associated invariant chain in rat stomach pyloric mucosa with *N*-methyl-*N'*-nitro-*N*-nitrosoguanidine exposure, Cancer Res. 1997; 57: 1416-8.
13 Oka M, Furihata C, Kitoh K, Yamamoto M, Ichinose M, Miki K, Ito T, Sakaki Y, Reske K, Involvement of dendritic cell response to resistance of stomach carcinogenesis caused by *N*-methyl-*N'*-nitro-*N*-nitrosoguanidine in rats, Cancer Res. 1998; 58: 4107-12.
14 Strano S, Dell'orso S, Di Agostino S, Fontemaggi G, Sacchi A, Blandino G. Mutant p53: an oncogenic transcription factor. Oncogene. 2007; 26: 2212-9.
15 Miled C, Pontoglio M, Garbay S, Yaniv M, Weitzman JB. A genomic map of p53 binding sites identifies novel *p53* targets involved in an apoptotic network. Cancer Res. 2005; 65: 5096-104.
16 Bates S, Rowan S, Vousden KH. Characterisation of human cyclin G1 and G2: DNA damage inducible genes. Oncogene. 1996; 13: 1103-9.
17 Burns TF, Samuels T, Winckler S, Korgaonkar C, Tompkins V, Horne MD, Quelle EE. Cyclin G1 has growth inhibitory activity linked to eh *ARF-Mdm2-p53* and *pRb* tumor suppressor pathways. Mol Cancer Res. 2003; 1: 195-205.
18 Menendez D, Inga A, Resnick MA. The biological impact of the human master regulator *p53* can be altered by mutations that change the spectrum and expression of its target genes. Mol Cell Biol. 2006; 26: 2297-308.
19 Alvarez S, Drane P, Meiller A, Bras M, Deguin-Chambon V, Bouvard V, May E. A comprehensive study of *p53* transcriptional activity in thymus and spleen of gamma irradiated mouse: high sensitivity of genes involved in the two main apoptotic pathways. Int J Radiat Biol. 2006; 82: 761-70.
20 Gao C, Zou Z, Xu L, Moul J, Seth P, Srivastava S. *p53*-dependent induction of heat shock protein 27 (*HSP27*) expression. Int J Cancer. 2000; 88: 191-4.
21 Burns TF, Fei P, Scata KA, Dicker DT, El-Deiry WS. Silencing of the novel p53 target gene *Snk/Plk2* leads to mitotic catastrophe in paclitaxel-exposed cells, Mol Cell Biol. 2003; 23: 5556-71.
22 Lee JS, Chu IS, Mikaelyan A, Calvisi DF, Heo J, Reddy JK, Thorgeirsson SS. Application of comparative functional genomics to identify best-fit mouse models to study human cancer. Nat Genet. 2004; 36: 1306-11.
23 Meyer K, Lee JS, Dyck PA, Cao WQ, Rao MS, Thorgeirsson SS, Reddy JK. Molecular profiling of hepatocellular carcinomas developing spontaneously in acyl-CoA oxidase deficient mice: comparison with liver tumors induced in wild-type mice by a peroxisome proliferator and a genotoxic carcinogen. Carcinogenesis. 2003; 24: 975-84.
24 Moto M, Okamura M, Muguruma M, Ito T, Jin M, Kashida Y, Mitsumori K. Gene expression analysis on the dicyclanil-induced hepatocellular tumors in mice. Toxicol Pathol. 2006; 34: 744-51.
25 Hokaiwado N, Asamoto M, Tsujimura K, Hirota T, Ichihara T, Satoh T, Shirai T. Rapid analysis of gene expression changes caused by liver carcinogens and chemopreventive agents using a newly developed three-dimensional microarray system. Cancer Sci. 2004; 95: 123-30.
26 Kier LD, Neft R, Tang L, Suizu R, Cook T, Onsurez K, Tiegler K, Sakai Y, Orvitz, Nolan T. Sankar U, Li AP. Applications of microarrays with toxicologically relevant genes (tox genes) for the evaluation of chemical toxicants in Sprague Dawley rats *in vivo* and human hepatocytes

in vitro. Mutat Res. 2004; 549: 101–13.

27 Stahl S, Ittrich C, Marx-Stoelting P, Köhle C, Ott T, Buchmann A, Schwarz M. Effect of the tumor promoter phenobarbital on the pattern of global gene expression in liver of connexin32-wild-type and connexin32-deficient mice. Int J Cancer. 2005; 115: 861–9.

28 Deaciuc IV, Doherty DE, Burikhanov R, Lee EY, Stromberg AJ, Peng X, de Villiers WJ. Large-scale gene profiling of the liver in a mouse model of chronic, intragastric ethanol infusion. J Hepatol. 2004; 40: 219–27.

HUMAN GENE THERAPY 18:74–80 (January 2007)

DOI: 10.1089/hum.2006.129

Technical Report

Rapid Construction of Small Interfering RNA-Expressing Adenoviral Vectors on the Basis of Direct Cloning of Short Hairpin RNA-Coding DNAs

HIROYUKI MIZUGUCHI,[1,2] NAOKO FUNAKOSHI,[1] TETSUJI HOSONO,[3] FUMINORI SAKURAI,[1] KENJI KAWABATA,[1] TERUHIDE YAMAGUCHI,[3] and TAKAO HAYAKAWA[4]

ABSTRACT

In the conventional method for constructing an adenoviral (Ad) vector expressing small interfering RNA (siRNA), short hairpin RNA (shRNA)-coding oligonucleotides are introduced downstream of a polymerase III (or polymerase II)-based promoter cloned into a shuttle plasmid. An siRNA expression cassette, which is cloned into the shuttle plasmid, is then introduced into the E1 deletion region of the Ad vector plasmid by *in vitro* ligation or homologous recombination in *Escherichia coli*, and the linearized plasmid is transfected into 293 cells, generating an Ad vector expressing siRNA. Therefore, two-step plasmid manipulation is required. In this study, we developed a method by which shRNA-coding oligonucleotides can be introduced directly into the Ad vector plasmid. To do this, we constructed a new vector plasmid into which the human U6 promoter sequence was cloned in advance. Unique restriction enzyme sites were introduced at the transcription start site of the U6 promoter sequence in the vector plasmid. Luciferase and p53 genes were efficiently knocked down by Ad vectors generated by the new method and expressing siRNA against the target gene. This method should be useful for RNA interference-based experiments, and should make it easy to construct an siRNA-expressing Ad vector library for functional screening.

INTRODUCTION

RNA INTERFERENCE (RNAi), which mediates the sequence-specific suppression of gene expression in a wide variety of eukaryotes by double-stranded RNA homologies to the target gene (Scherer and Rossi, 2003), is a powerful tool for the knockdown of gene expression. Transduction of synthetic small interfering RNA (siRNA; 19 to 29 nucleotides of RNA) or the promoter-based expression of siRNA in the cells results in sequence-dependent degradation of target mRNA and subsequent reduction of target gene expression. Most promoter-based RNAi systems express short hairpin RNA (shRNA), which is then trimmed by Dicer, generating functional siRNA. Polymerase III-based promoters, such as the small nuclear RNA U6 promoter or the human RNase P RNA H1 promoter, are widely used for the expression of shRNA (siRNA) (Scherer and Rossi, 2003), although polymerase II-based promoters are also used (Xia *et al.*, 2002; Shinagawa and Ishii, 2003). The promoter-based method has an advantage in that viral vectors as well as nonviral vectors can be used for delivery of the siRNA expression unit, whereas only nonviral vectors are used for delivery of synthetic siRNA.

Recombinant adenoviral (Ad) vectors have been used extensively to deliver foreign genes to a variety of cell types and tissues both *in vitro* and *in vivo* (McConnell and Imperiale, 2004; Volpers and Kochanek, 2004). They can be easily grown to high titers and can efficiently transfer genes into both dividing and nondividing cells. Therefore, Ad vector-mediated

[1]National Institute of Biomedical Innovation, Osaka 567-0085, Japan.
[2]Graduate School of Pharmaceutical Sciences, Osaka University, Osaka 567-0871, Japan.
[3]National Institute of Health Sciences, Tokyo 158-8501, Japan.
[4]Pharmaceuticals and Medical Devices Agency, Tokyo 100-0013, Japan.

delivery of an siRNA expression unit, in which a promoter-based shRNA expression cassette is delivered into the cell by the Ad vector, provides a valuable tool for both gene function studies and therapeutic applications.

Construction of Ad vectors used to be a time-consuming and labor-intensive procedure, but several improved methods to facilitate the construction of Ad vectors have been developed (reviewed in Mizuguchi *et al.*, 2001). The homologous recombination method in E1-complementing cell lines (i.e., 293 cells) has been the most widely used method for generating recombinant Ad vectors, and it has greatly contributed to the widespread use of Ad vectors (Bett *et al.*, 1994). The major limitations of this approach are the low frequency of the recombination event and the tedious and time-consuming plaque purification procedure required to select the recombinant virus of interest, because a relatively high percentage of the virus produced is wild type (in most cases, 20–70%), due to recombination with the Ad sequence integrated into the chromosomes of 293 cells. The improved *in vitro* ligation method (Mizuguchi and Kay, 1998, 1999) and the homologous recombination method in *Escherichia coli* (He *et al.*, 1998), which are commercially available from Clontech (Palo Alto, CA) and Invitrogen (Carlsbad, CA), respectively, have now become widely used, because these systems overcome the limitations of the homologous recombination method in 293 cells. To construct an Ad vector expressing siRNA by these two methods, shRNA-coding oligonucleotides are introduced downstream of the polymerase III (or polymerase II)-based promoter cloned in a shuttle plasmid. An shRNA (siRNA) expression cassette, which is cloned in the shuttle plasmid, is then introduced into the E1 deletion region of the Ad vector plasmid, which clones a full Ad genome, by simple *in vitro* ligation or homologous recombination in *E. coli*. The resulting plasmid is then linearized and transfected into 293 cells, generating an Ad vector expressing siRNA. Therefore, two-step *E. coli* transformation and plasmid manipulation is required for the improved *in vitro* ligation method, whereas three-step *E. coli* transformation and plasmid manipulation is required in the homologous recombination method in *E. coli* (because a special *E. coli* strain is used in the latter method, retransformation into a normal stain of *E. coli* is required) (reviewed in Mizuguchi *et al.*, 2001).

In the present study, we developed a simple method for generating an Ad vector expressing siRNA, in which shRNA-coding oligonucleotides could be directly introduced into an Ad vector plasmid containing the human U6 (hU6) promoter sequence. Unique restriction enzyme sites were introduced at the transcription start site of the hU6 promoter sequence cloned into the Ad vector plasmid. Two types of modified hU6 promoter sequence were constructed to develop this method. Using this method, only one-step *E. coli* transformation is required to generate an Ad vector plasmid containing an siRNA expression cassette.

MATERIALS AND METHODS

Cells

A549 and 293 cells were cultured in Dulbecco's modified Eagle's medium (DMEM) supplemented with 10% fetal calf serum (FCS). A549-Luc cells, which are stable transformants with luciferase expression, were cultured in DMEM supplemented with 10% FCS. For construction of A549-Luc cells, A549 cells were transfected with luciferase-expressing plasmid pGL3-Control-RSVneo, which contains the simian virus 40 (SV40) promoter/enhancer-luciferase cDNA-SV40 p(A) sequence and the neomycin expression cassette, using SuperFect transfection reagent (Qiagen, Valencia, CA). pGL3-Control-RSVneo was constructed by insertion of the Rous sarcoma virus (RSV) promoter-driven neomycin expression cassette into pGL3-Control (Promega, Madison, WI). Monoclonal A549 cells stably expressing luciferase (A549-Luc) were obtained by geneticin (G418) selection.

Plasmid and virus

The hU6 promoter sequence was amplified from human genomic DNA (Clontech), using the following primers: hU6-S1, hU6-AS1, and hU6-AS2 (Table 1). The hU6a and hU6b promoter sequences were amplified with hU6-S1/hU6-AS1 and hU6-S1/hU6-AS2 primer sets, respectively (see Fig. 2). These promoter sequences were introduced into pHM5 (Mizuguchi and Kay, 1999), and were then transferred into the E1 deletion region of the vector plasmid pAdHM4.1, a derivative of pAdHM4 (Mizuguchi and Kay, 1998) (the *Xba*I site outside the Ad genome of pAdHM4 was deleted), by an *in vitro* ligation method using the I-*Ceu*I and PI-*Sce*I sites (Mizuguchi and Kay, 1998, 1999), resulting in pAdHM4-hU6a and pAdHM4-hU6b, respectively (Fig. 1A). To construct a vector plasmid containing an shRNA-coding sequence against luciferase, oligonucleotides 1/2 and 3/4 were synthesized (Table 1), annealed, and cloned into the *Cla*I and *Xba*I sites of pAdHM4-hU6a or the *Swa*I and *Xba*I sites of pAdHM4-hU6b, generating pAdHM4-hU6a-Lu and pAdHM4-hU6b-Lu, respectively. The target sequence for siRNA is bp 158 to 176 of luciferase cDNA. For the construction of vector plasmid containing shRNA-coding sequence against p53 (Brummelkamp *et al.*, 2002), oligonucleotides 5/6 and 7/8 were used for cloning into the *Cla*I and *Xba*I sites of pAdHM4-hU6a or the *Swa*I and *Xba*I sites of pAdHM4-hU6b, generating pAdHM4-hU6a-p53 and pAdHM4-hU6b-p53, respectively. The target sequence for siRNA is bp 775 to 793 of human p53 cDNA.

The original intact hU6 promoter sequence, derived from an *Eco*RI/*Sal*I fragment of piGene hU6 (iGENE Therapeutics, Tsukuba, Japan), was also introduced into the *Sph*I and *Sal*I sites of pHM5 (Mizuguchi and Kay, 1999), resulting in pHM5-ihU6. pHM5-ihU6 was then digested with *Sal*I and *Xba*I, and ligated with oligonucleotides 9 and 10, resulting in pHM5-hU6. In this case, oligonucleotides 11/12 and 13/14 (for the shRNA-coding sequence against luciferase and p53, respectively) were introduced into the *Bsp*MI site of pHM5-hU6 according to the report of Miyagishi *et al.* (2004) and the manufacturer's instructions (iGENE Therapeutics); and then an siRNA expression cassette was inserted into the E1-deletion region of pAdHM4 (Mizuguchi and Kay, 1998), using the I-*Ceu*I and PI-*Sce*I sites, resulting in pAdHM4-hU6-Lu and pAdHM4-hU6-p53, respectively. The sequence was verified with a DNA sequencer (ABI PRISM 310: Applied Biosystems, Foster City, CA).

Viruses (Ad-hU6-Lu, Ad-hU6a-Lu, Ad-hU6b-Lu, Ad-hU6-p53, Ad-hU6a-p53, and Ad-hU6b-p53) were prepared by the

TABLE 1. OLIGONUCLEOTIDES USED IN THE PRESENT STUDY

Oligonucleotide	*Sequence of oligonucleotide (5′–3′)*
hU6-S1 primer	aaggtcgggcaggaagagggcctа
hU6-AS1 primer	ggtctagaagt*atcgat*ttcgtctttccacaagatatat (*Xba*I and *Cla*I recognition sequences are underlined and italicized, respectively)
hU6-AS2 primer	ggtctagaagt*atttaaat*cgtcctttccacaagatatataa (*Xba*I and *Swa*I recognition sequences are underlined and italicized, respectively)
Oligonucleotide 1	cg*acgctgagtacttcgaaat*ttcaagaga*atttcgaagtactcagcgt*ttttttggaaat (loop sequences and siRNA-coding sequence are underlined and italicized, respectively)
Oligonucleotide 2	ctagatttccaaaaaa*acgctgagtacttcgaaat*tctcttgaa*atttcgaagtactcagcgt* (loop sequences and siRNA-coding sequence are underlined and italicized, respectively)
Oligonucleotide 3	cc*acgctgagtacttcgaaat*ttcaagaga*atttcgaagtactcagcgt*ttttttggaaat (loop sequences and siRNA-coding sequence are underlined and italicized, respectively)
Oligonucleotide 4	ctagatttccaaaaaa*acgctgagtacttcgaaat*tctcttgaa*atttcgaagtactcagcgtgg* (loop sequences and siRNA-coding sequence are underlined and italicized, respectively)
Oligonucleotide 5	cg*gactccagtggtaatctac*ttcaagaga*gtagattaccactggagtc*ttttttggaaat (loop sequences and siRNA-coding sequence are underlined and italicized, respectively)
Oligonucleotide 6	ctagatttccaaaaaa*gactccagtggtaatctac*tctcttgaa*gtagattaccactggagtc* (loop sequences and siRNA-coding sequence are underlined and italicized, respectively)
Oligonucleotide 7	cc*gactccagtggtaatctac*ttcaagaga*gtagattaccactggagtc*ttttttggaaat (loop sequences and siRNA-coding sequence are underlined and italicized, respectively)
Oligonucleotide 8	ctagatttccaaaaaa*gactccagtggtaatctac*tctcttgaa*gtagattaccactggagtc*gg (loop sequences and siRNA-coding sequence are underlined and italicized, respectively)
Oligonucleotide 9	tcgacctgcaggcatgcaagcttc (BspMI recognition sequences are underlined)
Oligonucleotide 10	ctaggaagcttgcatgcctgcagg (BspMI recognition sequences are underlined)
Oligonucleotide 11	cacc*acgctgagtacttcgaaat*ttcaagaga*atttcgaagtactcagcgt*ttttt (loop sequences and siRNA-coding sequence are underlined and italicized, respectively)
Oligonucleotide 12	gcataaaaaa*acgctgagtacttcgaaat*tctcttgaa*atttcgaagtactcagcgt* (loop sequences and siRNA-coding sequence are underlined and italicized, respectively)
Oligonucleotide 13	cacc*gactccagtggtaatctac*ttcaagaga*gtagattaccactggagtc*ttttttt (loop sequences and siRNA-coding sequence are underlined and italicized, respectively)
Oligonucleotide 14	gcataaaaa*gactccagtggtaatctac*tctcttgaa*gtagattaccactggagtc* (loop sequences and siRNA-coding sequence are underlined and italicized, respectively)

transfection of a *Pac*I-linearized vector plasmid (pAdHM4-hU6-Lu, pAdHM4-hU6a-Lu, pAdHM4-hU6b-Lu, pAdHM4-hU6-p53, pAdHM4-hU6a-p53, and pAdHM4-hU6b-p53, respectively) into 293 cells as described previously (Mizuguchi and Kay, 1998). Ad vectors containing only the original intact hU6 promoter sequence (without a target sequence; Ad-hU6) were similarly constructed with pHM5-hU6 and pAdHM4. The virus was purified by $CsCl_2$ gradient centrifugation; dialyzed with a solution containing 10 m*M* Tris (pH 7.5), 1 m*M* $MgCl_2$, and 10% glycerol; and stored in aliquots at −70°C. Determination of virus particle (VP) titers and infectious titers was accomplished spectrophotometrically by the method of Maizel *et al.* (1968) and with an Adeno-X rapid titer kit (Clontech), respectively. The infectious titer-to-particle ratio was 1:36 for Ad-hU6, 1:31 for Ad-hU6-Lu, 1:28 for Ad-hU6a-Lu, 1:24 for Ad-hU6b-Lu, 1:22 for Ad-hU6-p53, 1:12 for Ad-hU6a-p53, and 1:15 for Ad-hU6b-p53.

Adenovirus-mediated gene transduction and luciferase assay

A549 cells (2×10^5 cells) were seeded into a 12-well dish. The next day, they were transduced with the Ad vectors for 1.5 hr. Determination of luciferase production in the cells and extraction of cellular protein for Western blotting were performed after a 72-hr culture period. Luciferase production in the cells was measured with a luciferase assay system (PicaGene LT 2.0; produced by Toyo Ink [Tokyo, Japan] for Wako [Kyoto, Japan])

Western blotting for p53

Cell extracts were prepared in lysis buffer (25 m*M* Tris [pH 7.5], 1% Triton X-100, 0.5% sodium deoxycholate, 5 m*M* EDTA, 150 m*M* NaCl) containing a cocktail of protease inhibitors (Sigma, St. Louis, MO). The protein content was measured

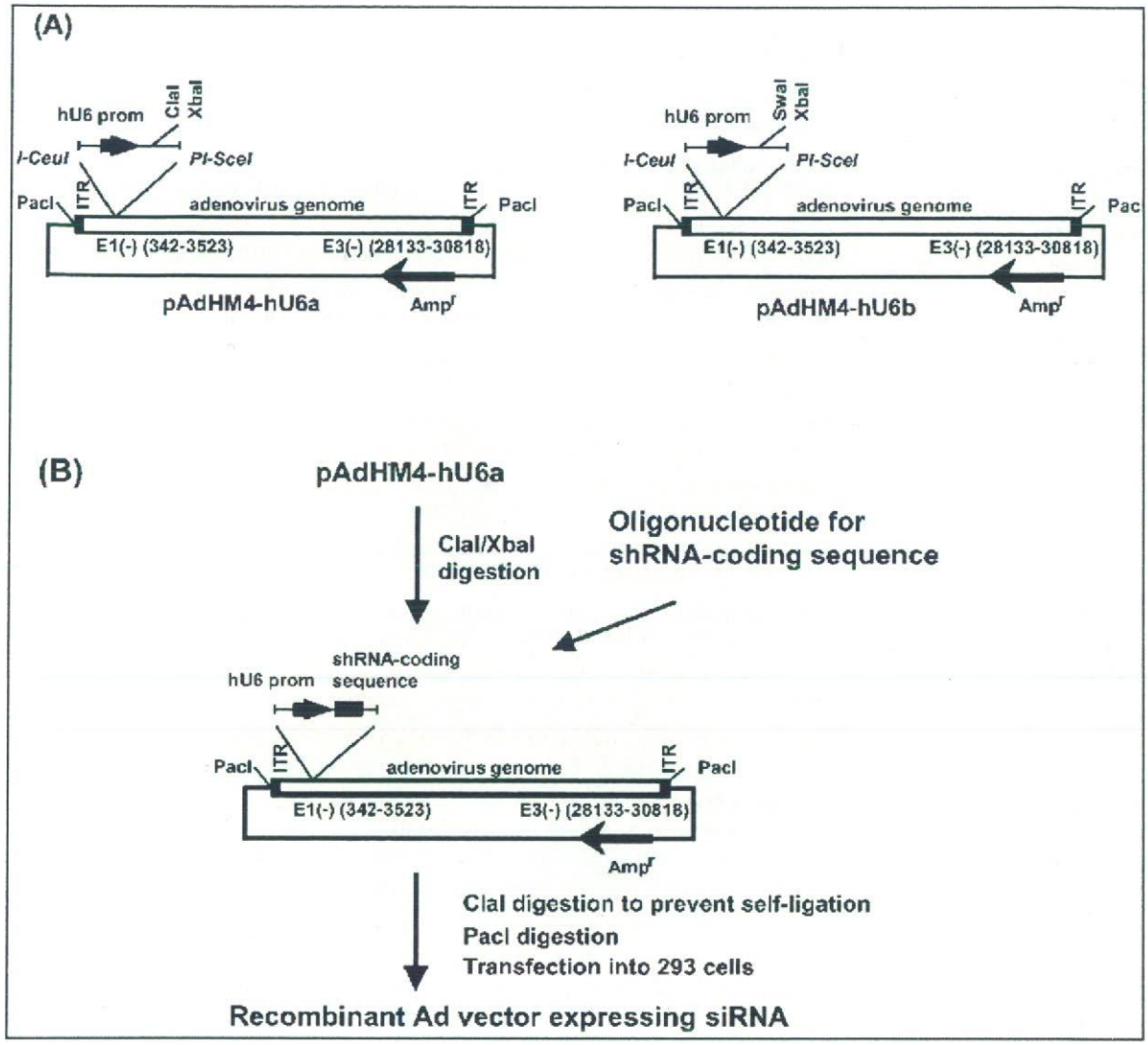

FIG. 1. Vector plasmids and the construction strategy for Ad vectors expressing siRNA. (**A**) Vector plasmids pAdHM4-hU6a and pAdHM4-hU6b. pAdHM4-hU6a contains a unique *Cla*I site at the transcription start site of the hU6 promoter sequence and an *Xba*I site downstream from the promoter sequence. pAdHM4-hU6b contains a unique *Swa*I site at the transcription start site of the hU6 promoter sequence and an *Xba*I site downstream from the promoter sequence. (**B**) Construction strategy for the Ad vector expressing siRNA. pAdHM4-hU6a was digested with *Cla*I/*Xba*I and ligated with oligonucleotides for the shRNA-coding sequence. Ligation products were then digested with *Cla*I to prevent the generation of nonrecombinant parental plasmid. The resulting plasmid was linearized by digestion with *Pac*I and transfected into 293 cells, generating recombinant Ad vectors expressing siRNA. pAdHM4-hU6b was similarly used.

with a Bio-Rad assay kit (Bio-Rad, Hercules, CA), using bovine serum albumin as the standard. Protein samples (10 μg) were electrophoresed on sodium dodecyl sulfate (SDS)– 12.5% polyacrylamide gels under reducing conditions, followed by electrotransfer to Immobilon-P membranes (Millipore, Bedford, MA). After blocking in nonfat dry milk, the filters were incubated with antibodies against p53 (Santa Cruz Biotechnology, Santa Cruz, CA) and actin (Oncogene Research Products/EMD Biosciences, San Diego, CA), followed by incubation in the presence of peroxidase-labeled goat anti-mouse IgG antibody (American Qualex Antibodies, San Clemente, CA) or peroxidase-labeled goat anti-mouse IgM antibody (Oncogene Research Products/EMD Biosciences). The filters were developed by chemiluminescence (ECL Western blotting detection system; GE Healthcare, Piscataway, NJ). The signals were read with an LAS-3000 (Fujifilm, Tokyo, Japan), and quantified with Image Gauge software (Fujifilm).

RESULTS AND DISCUSSION

Rapid and efficient construction of Ad vectors expressing siRNA offers the promise of using RNAi in the context of both gene function analysis and therapeutic applications. In the present study, we developed a simple method for constructing Ad vectors expressing siRNA, based on only one-step *in vitro* ligation. To do this, we first constructed an Ad vector plasmid containing the E1- and E3-deleted Ad genome and the hU6 pro-

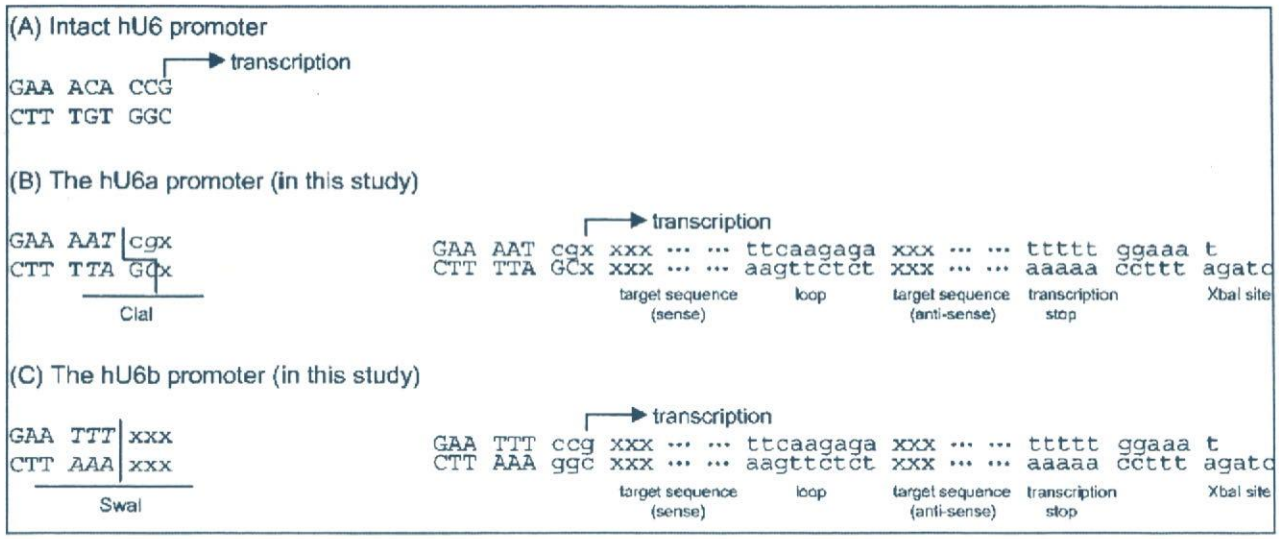

FIG. 2. Sequences at the transcription start site of the new hU6 promoter. (**A**) Intact hU6 promoter sequence. (**B**) hU6a promoter sequence. In this promoter, the *Cla*I site is placed at the transcription start site. (**C**) hU6b promoter sequence. In this promoter, a *Swa*I site is placed at the transcription start site. shRNA-coding oligonucleotides to be synthesized for each promoter are shown as lower-case letters on the right-hand side.

moter sequence in the E1 deletion region, pAdHM4-hU6a and pAdHM4-hU6b (Fig. 1A). By introducing the hU6 promoter sequence into the vector plasmid in advance, the cloning step of the gene of interest from the shuttle plasmid to the vector plasmid, which is an essential step in the conventional method for constructing Ad vectors (namely, the improved *in vitro* ligation method [Mizuguchi and Kay, 1998, 1999] and homologous recombination method in *E. coli* [He *et al.*, 1998]), can be skipped. To make it possible to directly clone the shRNA-coding oligonucleotides downstream of the hU6 promoter sequence, hU6 promoters containing unique restriction enzyme sites at the transcription start site have been developed. The new hU6 promoter sequences contain a *Cla*I or *Swa*I site around the transcription start site and an *Xba*I site downstream from the promoter (Figs. 1 and 2). These enzyme sites were selected because they do not cut the E1- and E3-deleted Ad genome. Because the transcription of shRNA might be influenced by the mutated sequences around the transcription start site, two types of hU6 promoters, differing by only a few nucleotides, were constructed. The hU6a promoter sequence contains a *Cla*I site, whereas the hU6b promoter sequence contains a *Swa*I site. *Cla*I, *Swa*I, and *Xba*I sites are unique in the vector plasmids pAdHM4-hU6a and pAdHM4-hU6b. To generate a recombinant vector plasmid for Ad vectors expressing siRNA, oligonucleotides for shRNA against the target gene were synthesized, annealed, and ligated with *Cla*I/*Xba*I-digested pAdHM4-hU6a or *Swa*I/*Xba*I-digested pAdHM4-hU6b. Oligonucleotides were designed so that recombinant vector plasmid containing the shRNA-coding sequence is redigested with *Xba*I, but not with *Cla*I or *Swa*I. By designing oligonucleotides like the one described above, the generation of self-ligated plasmid can be avoided by digestion of the ligation products with *Cla*I or *Swa*I. On the right side of Fig. 2, DNA sequences, including the shRNA-coding sequence around the transcription start site of the hU6 promoter, are shown. Oligonucleotides that must be synthesized for the shRNA-coding sequence are shown as lower-case letters. By using the method developed in the present study, we could easily generate Ad vectors expressing siRNAs against luciferase and human p53. More than 90% of the recombinant Ad vector plasmids contained the correct insert. Because the *Cla*I- (or *Swa*I-) and *Xba*I-digested pAdHM4-hU6a and pAdHM4-hU6b can be stored at −20°C, only the ligation-based introduction of oligonucleotides into these sites of the vector plasmid would be required for the construction of an appropriate vector.

To examine the function of Ad vectors expressing siRNA against luciferase (Ad-hU6a-Lu and Ad-hU6b-Lu), the efficiency of knockdown of luciferase expression in A549-Luc cells, which stably express luciferase, was examined by treatment with Ad-hU6a-Lu or Ad-hU6b-Lu (Fig. 3). Ad-hU6-Lu, in which the hU6 promoter contains the original intact sequence even after introduction of an shRNA-coding sequence, was used as a positive control. To generate Ad-hU6-Lu, the shRNA-coding sequence was first introduced downstream from the hU6 promoter sequence cloned into the shuttle plasmid, according to the report of Miyagishi *et al.* (2004) and the manufacturer's instructions (iGENE Therapeutics); the shRNA expression cassette was then introduced into the E1 deletion region of the Ad vector plasmid pAdHM4 (Mizuguchi and Kay, 1998). Transfection of a *Pac*I-digested vector plasmid into 293 cells generated Ad-hU6-Lu. Ad-hU6, which contains the intact hU6 promoter without the shRNA-coding sequence, and Ad-hU6-p53, which contains the intact hU6 promoter with the shRNA-coding sequence against human p53, were similarly constructed and used as negative controls. Data showed that Ad-hU6a-Lu and Ad-hU6b-Lu suppressed luciferase expression in A549-Luc cells as efficiently as Ad-hU6-Lu, in a dose-dependent manner (Fig. 3). Ad-hU6 and Ad-hU6-p53 showed no effects on luciferase expression. Ad-hU6a-p53 and Ad-hU6b-p53 (these Ad vectors are used in Fig. 4) also had no influence on luciferase expression (data not shown). The RNAi effect of luciferase expression was relatively weak compared with that of p53 (de-

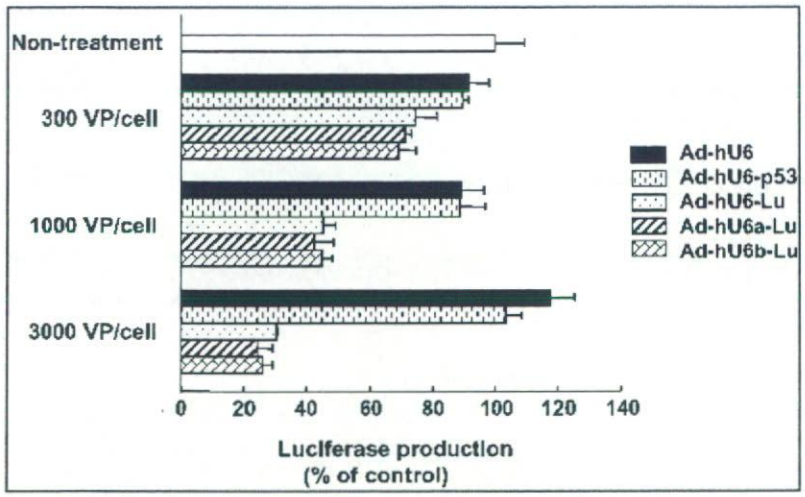

FIG. 3. Suppression of luciferase expression by Ad vector expressing siRNA. A549-Luc cells, which stably express luciferase, were transduced for 1.5 hr with Ad-hU6, Ad-hU6-p53, Ad-hU6-Lu, Ad-hU6a-Lu, or Ad-hU6b-Lu at 300, 1000, or 3000 VP/cell. After culturing for 72 hr, luciferase production in the cells was measured by luminescence assay. Data are expressed as means and SD ($n = 4$).

scribed below). This difference probably occurred because the A549-Luc cells were expressing luciferase from a strong viral promoter (SV40 promoter and enhancer) and because the levels of luciferase expression were higher than those of endogenous p53 expression.

We next examined the RNAi effect of the siRNA-expressing Ad vector generated in the present study on the endogenous gene. As a model, we silenced p53 expression in A549 cells (Fig. 4). Ad-hU6a-p53 and Ad-hU6b-p53 were generated, and Ad-hU6, Ad-hU6-Lu, and Ad-hU6-p53 were also used. Ad-hU6-p53 contains the intact hU6 promoter sequence, including the transcription start site, even after introduction of the shRNA-coding sequence. A549 cells were transduced with a 300- or 1000-VP/cell of each Ad vector, and cultured for 3 days. Levels of p53 expression were examined by Western blotting. Expression of actin was also measured as an internal control. Expression of p53 in A549 cells was efficiently decreased by treatment with Ad-hU6a-p53 and Ad-hU6b-p53 as well as with Ad-hU6-p53. Levels of p53 expression in cells treated with Ad-hU6-p53, Ad-hU6a-p53, or Ad-hU6b-p53 at 1000 VP/cell were decreased to 7, 2, and 5%, respectively, relative to cells treated with Ad-hU6, according to Image Gauge software (Fujifilm) (in the case of 300 VP/cell, they were decreased to 53, 24, and 30%, respectively). The efficiency of p53 silencing by treatment with Ad-hU6-p53 was slightly lower than that with Ad-hU6a-p53 or Ad-hU6b-p53. This reduced efficiency is likely due to the approximately 1.5 to 2 times lower infectious titer-to-particle titer ratio of Ad-hU6-p53 in comparison with those of Ad-hU6a-p53 and Ad-hU6b-p53. Ad-hU6 and Ad-hU6-Lu did not decrease the level of p53 expression (Fig. 4). These results indicate that new hU6 promoters containing *Cla*I or *Swa*I sites at the transcription start site should transcribe as efficiently as the original hU6 promoter, and that Ad vectors containing the new hU6 promoters efficiently silence target gene expression. Different vector systems (pAdHM4-hU6a and pAdHM4-hU6b) should be used according to the specific purpose.

To facilitate the construction of an siRNA expression plasmid, the U6 and H1 promoters, which contain *Apa*I, *Bbs*I, *Bgl*II, *Eco*RV, *Sal*I, and *Xba*I sites, etc., at the transcription start site, have been developed (Brummelkamp *et al.*, 2002; Lee *et al.*, 2002; Paddison *et al.*, 2002; Paul *et al.*, 2002; Sui *et al.*, 2002; Yu *et al.*, 2002; Boden *et al.*, 2003). All types of promoters worked efficiently, and could be widely used for efficient RNAi, although the efficiency (activity) of the mutated promoters described above has not been compared with that of the intact promoter. The present study clearly showed that the mutated hU6 promoter, at least one having a *Cla*I or *Swa*I site at the transcription start site and an *Xba*I site downstream of the promoter sequence, is similar in activity to the intact hU6 promoter and would not influence the function of the promoter.

The method using polymerase chain reaction (PCR)-based amplification of shRNA together with the U6 promoter followed by subsequent cloning of the complete expression cassette directly into the Ad vector genome is another strategy for one-step construction of recombinant Ad plasmids containing an siRNA expression cassette. In this method, however, the procedures described below are required for preparation of insert DNA: (1) ordering of the PCR primer, (2) PCR, (3) purification of the PCR product, (4) restriction enzyme digestion and purification of the PCR product, and (5) ligation. In our present system, only the following procedures are required: (1) ordering of the oligonucleotides, (2) hybridization of the oligonucleotides, and (3) ligation. Thus, the present method would be much easier and would allow any laboratory to easily construct

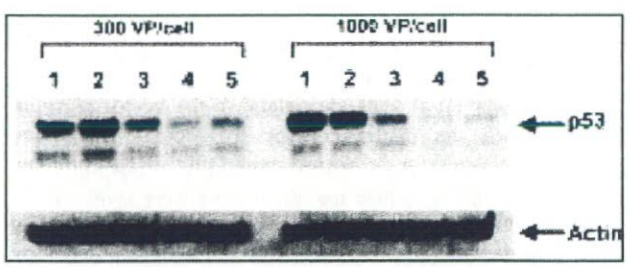

FIG. 4. Suppression of human p53 expression by Ad vector expressing siRNA. A549 cells were transduced for 1.5 hr with Ad-hU6 (lane 1), Ad-hU6-Lu (lane 2), Ad-hU6-p53 (lane 3), Ad-hU6a-p53 (lane 4), or Ad-hU6b-p53 (lane 5) at 300 or 1000 VP/cell, and then cultured for 3 days. Proteins were then extracted from the cells, and the levels of p53 expression were examined by Western blotting. The actin bands served as an internal control for equal total protein loading. The extra (lower) bands of p53 are nonspecific.

Ad vectors expressing siRNA for gene transfer studies and therapeutic applications.

Various types of promoters that are based on polymerase II as well as polymerase III have been developed to transcribe shRNA (siRNA) (Xia *et al.*, 2002; Shinagawa and Ishii, 2003). Although the present study applied the most commonly used U6 promoter for simple and efficient construction of siRNA-expressing Ad vectors, this method could easily be applied to vectors using other promoters including polymerase II-based promoters. This method can also easily be combined with various types of improved Ad vectors, such as Ad vectors containing capsid modification (Koizumi *et al.*, 2003, 2006; Mizuguchi and Hayakawa, 2004; Kurachi *et al.*, 2006) or Ad vectors belonging to different subgroups to modify tropism (Sakurai *et al.*, 2003), and Ad vectors containing a tetracycline-inducible RNAi system (Hosono *et al.*, 2004). The method developed in the present study should be a powerful tool for the application of RNAi, and might facilitate the development of an siRNA-expressing Ad vector library for functional screening.

ACKNOWLEDGMENTS

The authors thank Risako Nagahashi-Nakano and Tomomi Sasaki for technical assistance. This work was supported by grants from the Ministry of Health, Labor, and Welfare of Japan.

REFERENCES

BETT, A.J., HADDARA, W., PREVEC, L., and GRAHAM, F.L. (1994). An efficient and flexible system for construction of adenovirus vectors with insertions or deletions in early regions 1 and 3. Proc. Natl. Acad. Sci. U.S.A. **91,** 8802–8806.

BODEN, D., PUSCH, O., LEE, F., TUCKER, L., SHANK, P.R., and RAMRATNAM, B. (2003). Promoter choice affects the potency of HIV-1 specific RNA interference. Nucleic Acids Res. **31,** 5033–5038.

BRUMMELKAMP, T.R., BERNARDS, R., and AGAMI, R. (2002). A system for stable expression of short interfering RNAs in mammalian cells. Science **296,** 550–553.

HE, T.C., ZHOU, S., DA COSTA, L.T., YU, J., KINZLER, K.W., and VOGELSTEIN, B. (1998). A simplified system for generating recombinant adenoviruses. Proc. Natl. Acad. Sci. U.S.A. **95,** 2509–2514.

HOSONO, T., MIZUGUCHI, H., KATAYAMA, K., XU, Z.L., SAKURAI, F., ISHII-WATABE, A., KAWABATA, K., YAMAGUCHI, T., NAKAGAWA, S., MAYUMI, T., and HAYAKAWA, T. (2004). Adenovirus vector-mediated doxycycline-inducible RNA interference. Hum. Gene Ther. **15,** 813–819.

KOIZUMI, N., MIZUGUCHI, H., UTOGUCHI, N., WATANABE, Y., and HAYAKAWA, T. (2003). Generation of fiber-modified adenovirus vectors containing heterologous peptides in both the HI loop and C terminus of the fiber knob. J. Gene Med. **5,** 267–276.

KOIZUMI, N., KAWABATA, K., SAKURAI, F., WATANABE, Y., HAYAKAWA, T., and MIZUGUCHI, H. (2006). Modified adenoviral vectors ablated for coxsackievirus–adenovirus receptor, α_v integrin, and heparan sulfate binding reduce *in vivo* tissue transduction and toxicity. Hum. Gene Ther. **17,** 264–279.

KURACHI, S., KOIZUMI, N., SAKURAI, F., KAWABATA, K., SAKURAI, H., NAKAGAWA, S., HAYAKAWA, T. and MIZUGUCHI, H. (2006). Characterization of capsid-modified adenovirus vectors containing heterologous peptides in the fiber knob, protein IX, or hexon. Gene Ther. (in press).

LEE, N.S., DOHJIMA, T., BAUER, G., LI, H., LI, M.J., EHSANI, A., SALVATERRA, P., and ROSSI, J. (2002). Expression of small interfering RNAs targeted against HIV-1 *rev* transcripts in human cells. Nat. Biotechnol. **20,** 500–505.

MAIZEL, J.V., Jr., WHITE, D.O., and SCHARFF, M.D. (1968). The polypeptides of adenovirus. I. Evidence for multiple protein components in the virion and a comparison of types 2, 7A, and 12. Virology **36,** 115–125.

McCONNELL, M.J., and IMPERIALE, M.J. (2004). Biology of adenovirus and its use as a vector for gene therapy. Hum. Gene Ther. **15,** 1022–1033.

MIYAGISHI, M., SUMIMOTO, H., MIYOSHI, H., KAWAKAMI, Y., and TAIRA, K. (2004). Optimization of an siRNA-expression system with an improved hairpin and its significant suppressive effects in mammalian cells. J. Gene Med. **6,** 715–723.

MIZUGUCHI, H., and HAYAKAWA, T. (2004). Targeted adenovirus vectors. Hum. Gene Ther. **15,** 1034–1044.

MIZUGUCHI, H., and KAY, M.A. (1998). Efficient construction of a recombinant adenovirus vector by an improved *in vitro* ligation method. Hum. Gene Ther. **9,** 2577–2583.

MIZUGUCHI, H., and KAY, M.A. (1999). A simple method for constructing E1- and E1/E4-deleted recombinant adenoviral vectors. Hum. Gene Ther. **10,** 2013–2017.

MIZUGUCHI, H., KAY, M.A., and HAYAKAWA, T. (2001). Approaches for generating recombinant adenovirus vectors. Adv. Drug Deliv. Rev. **52,** 165–176.

PADDISON, P.J., CAUDY, A.A., BERNSTEIN, E., HANNON, G.J., and CONKLIN, D.S. (2002). Short hairpin RNAs (shRNAs) induce sequence-specific silencing in mammalian cells. Genes Dev. **16,** 948–958.

PAUL, C.P., GOOD, P.D., WINER, I., and ENGELKE, D.R. (2002). Effective expression of small interfering RNA in human cells. Nat. Biotechnol. **20,** 505–508.

SAKURAI, F., MIZUGUCHI, H., and HAYAKAWA, T. (2003). Efficient gene transfer into human $CD34^+$ cells by an adenovirus type 35 vector. Gene Ther. **10,** 1041–1048.

SCHERER, L.J., and ROSSI, J.J. (2003). Approaches for the sequence-specific knockdown of mRNA. Nat. Biotechnol. **21,** 1457–1465.

SHINAGAWA, T., and ISHII, S. (2003). Generation of Ski-knockdown mice by expressing a long double-strand RNA from an RNA polymerase II promoter. Genes Dev. **17,** 1340–1345.

SUI, G., SOOHOO, C., AFFAR EL, B., GAY, F., SHI, Y., and FORRESTER, W.C. (2002). A DNA vector-based RNAi technology to suppress gene expression in mammalian cells. Proc. Natl. Acad. Sci. U.S.A. **99,** 5515–5520.

VOLPERS, C., and KOCHANEK, S. (2004). Adenoviral vectors for gene transfer and therapy. J. Gene Med. **6,** S164–S171.

XIA, H., MAO, Q., PAULSON, H.L., and DAVIDSON, B.L. (2002). siRNA-mediated gene silencing *in vitro* and *in vivo*. Nat. Biotechnol. **20,** 1006–1010.

YU, J.Y., DERUITER, S.L., and TURNER, D.L. (2002). RNA interference by expression of short-interfering RNAs and hairpin RNAs in mammalian cells. Proc. Natl. Acad. Sci. U.S.A. **99,** 6047–6052.

Address reprint requests to:
Dr. Hiroyuki Mizuguchi
National Institute of Biomedical Innovation
Asagi 7-6-8, Saito
Ibaraki, Osaka 567-0085, Japan

E-mail: mizuguch@nibio.go.jp

Received for publication September 3, 2006; accepted after revision November 12, 2006.

Published online: December 22, 2006.

THE JOURNAL OF BIOLOGICAL CHEMISTRY VOL. 282, NO. 46, pp. 33507–33514, November 16, 2007

A New Role of Thrombopoietin Enhancing *ex Vivo* Expansion of Endothelial Precursor Cells Derived from AC133-positive Cells*

Received for publication, May 14, 2007, and in revised form, September 5, 2007 Published, JBC Papers in Press, September 7, 2007, DOI 10.1074/jbc.M703919200

Toshie Kanayasu-Toyoda[‡], Akiko Ishii-Watabe[‡], Takayoshi Suzuki[§], Tadashi Oshizawa[§], and Teruhide Yamaguchi[‡1]

From the Divisions of [‡]Biological Chemistry and Biologicals, and [§]Cellular and Gene Therapy Products, National Institute of Health Sciences, Kamiyoga 1-18-1, Setagayaku, Tokyo 158-8501, Japan

We previously reported that CD31^{bright} cells, which were sorted from cultured AC133$^+$ cells of adult peripheral blood cells, differentiated more efficiently into endothelial cells than CD31$^+$ cells or CD31$^-$ cells, suggesting that CD31^{bright} cells may be endothelial precursor cells. In this study, we found that CD31^{bright} cells have a strong ability to release cytokines. The mixture of vascular endothelial growth factor (VEGF), thrombopoietin (TPO), and stem cell factor stimulated *ex vivo* expansion of the total cell number from cultured AC133$^+$ cells of adult peripheral blood cells and cord blood cells, resulting in incrementation of the adhesion cells, in which endothelial nitric oxide synthase and kinase insert domain-containing receptor were positive. Moreover, the mixture of VEGF and TPO increased the CD31^{bright} cell population when compared with VEGF alone or the mixture of VEGF and stem cell factor. These data suggest that TPO is an important growth factor that can promote endothelial precursor cells expansion *ex vivo*.

Neovascularization is an important adaptation to rescue tissue from critical ischemia. Postnatal blood vessel formation was formerly thought to be primarily due to the migration and proliferation of preexisting, fully differentiated endothelial cells, a process referred to as angiogenesis. Recent studies provide increasing evidence that circulating bone marrow-derived endothelial progenitor cells (EPCs)[2] contribute substantially to adult blood vessel formation (1–5). Cell therapy using EPCs is widely performed to rescue tissue damaged due to critical ischemia.

Although EPCs have been thought to be derived from many kinds of cells, cells characterized as CD34$^+$ (6), AC133$^+$ (7, 8), and CD14$^+$ (9) are also thought to differentiate to EPCs. The main role of EPCs has been thought to be the release of angiogenic factors such as interleukin-8 (IL-8), granulocyte colony-stimulating factor (G-CSF), hepatocyte growth factor, and vascular endothelial growth factor (VEGF) (9). To obtain a sufficient number of EPCs for the treatment may be very important in cell therapy for critical ischemia.

On the other hand, EPCs are mobilized from bone marrow by many substances such as G-CSF (10), granulocyte macrophage-colony stimulating factor (GM-CSF) (5), VEGF (3), erythropoietin (11–13), and statins (14, 15) *in vivo*. To get as many EPCs as possible without unduly burdening the patient, it is desirable to establish efficient expansion methods for EPCs *in vitro*.

Thrombopoietin (TPO), initially identified as the primary regulator of platelet production (16), plays an important and nonredundant role in the self-renewal of and expansion methods for hematopoietic stem cells (17–19). Recently, TPO has been found to exert a proangiogenic effect on cultured endothelial cells (20). The mechanism by which hematopoietic cytokines support revascularization *in vivo*, however, remains unknown. TPO has increased the number of colony-forming units-granulocyte-macrophage (21) and of burst-forming units-erythroid (22) *in vivo* and leads to a redistribution of colony-forming units-erythroid from marrow to spleen. Moreover, TPO acts in synergy with erythropoietin to increase the growth of burst-forming units-erythroid and the generation of colony-forming units-erythroid from marrow cells (21, 23, 24).

In our previous study (25), we isolated AC133$^+$ cells and examined their endothelial differentiation *in vitro*. CD31(PECAM-1)$^+$ and CD31^{bright} cells appeared at an early stage of the *in vitro* differentiation of AC133$^+$ cells, and CD31^{bright} cells derived from AC133$^+$ cells were identified as the precursors of endothelial cells because CD31^{bright} cells had differentiated more efficiently to endothelial cells than others. Therefore, we conclude that CD31^{bright} cells derived from AC133$^+$ cells possess the typical character of EPCs. In this study, we analyzed the effects of TPO on the appearance of CD31^{bright} cells from AC133$^+$ cells, and we show that TPO plays an important role in *in vitro* EPC expansion.

EXPERIMENTAL PROCEDURES

Reagents—Recombinant TPO and recombinant stem cell factor (SCF) were kindly provided by Kirin-Amgen Inc. (Thousand Oaks, CA). Recombinant human VEGF was purchased from Strathmann Biotec AG (Hamburg, Germany). The AC133

* This work was supported in part by a grant-in-aid for health and labor science research from the Japanese Ministry of Health, Labor, and Welfare, and in part by a grant-in-aid for Research on Health Sciences focusing on Drug Innovation from the Japan Health Sciences Foundation. The costs of publication of this article were defrayed in part by the payment of page charges. This article must therefore be hereby marked "*advertisement*" in accordance with 18 U.S.C. Section 1734 solely to indicate this fact.

[1] To whom correspondence should be addressed. Tel.: 81-3-3700-9064; Fax: 81-3-3707-6950; E-mail: yamaguch@nihs.go.jp.

[2] The abbreviations used are: EPCs, endothelial precursor cells; VEGF, vascular endothelial growth factor; FN, fibronectin; PBS, phosphate-buffered saline; FITC, fluorescein isothiocyanate; PE, phycoerythrin; TPO, thrombopoietin; SCF, stem cell factor; G-CSF, granulocyte colony-stimulating factor; GM-CSF, granulocyte macrophage-colony stimulating factor; IL, interleukin; PI3K, phosphatidylinositol 3-kinase; VEcad, vascular endothelial cadherin; eNOS, endothelial nitric oxide synthase; FBS, fetal bovine serum; STAT, signal transducers and activators of transcription; JAK, Janus kinase; KDR, kinase insert domain-containing receptor.

magnetic cell sorting kit and phycoerythrin (PE)-conjugated anti-CD133/2 antibody were from Miltenyi Biotec (Gladbach, Germany). Allophycocyanin-conjugated anti-CD110 (TPO receptor) antibody, fluorescein isothiocyanate (FITC)-conjugated anti-CD31 monoclonal antibody, FITC-conjugated anti-CD34 monoclonal antibody, and anti-STAT3 monoclonal antibody were from Pharmingen. Phycoerythrin-conjugated vascular endothelial cadherin (VEcad/CD144) antibody was from Beckman Coulter (Marseilles, France). Anti-vascular endothelial growth factor receptor-2 (Flk-1/KDR) monoclonal antibody (Santa Cruz Biotechnology, Inc., Santa Cruz, CA) and anti-human endothelial nitric oxide synthase (eNOS) rabbit polyclonal antibody (Cayman Chemical, Ann Arbor, MI) were obtained. Anti-phospho-Akt (Ser-473) antibody, anti-Akt antibody, and anti-phospho-STAT3 (Tyr-705) antibody were from Cell Signaling Technology (Beverly, MA). Fibronectin (FN)- and type IV collagen-coated dishes were purchased from Iwaki Co., Tokyo, Japan. Phycoerythrin-conjugated anti-CD14 antibody was from DakoCytomation (Glostrup, Denmark).

Preparation of Peripheral Blood Mononuclear Cells—Human cord blood was kindly supplied by the Metro Tokyo Red Cross Cord Blood Bank (Tokyo, Japan) with informed consent. The buffy coat fraction was prepared from voluntary donated human blood of Saitama Red Cross of Japan (Saitama, Japan). The blood sample was diluted with phosphate-buffered saline (PBS) containing 2 mM EDTA and was loaded on a Lymphoprep™ tube (Axis-Shield PoC AS, Oslo Norway) (density = 1.077). After being centrifuged for 20 min 800 × *g* at 18 °C, mononuclear cells were collected and washed with sorting solution (PBS supplemented with 2 mM EDTA and 0.5% bovine serum albumin).

Flow Cytometric Analysis of AC133 and CD34 Expression in Mononuclear Cells—To eliminate the dead cells, dead cells were stained with 7-amino actinomycin D. Mononuclear cells were labeled with PE-conjugated anti-AC133 monoclonal antibody and FITC-conjugated anti-CD34 monoclonal antibody simultaneously at 4 °C for 30 min. After washing with the sorting solution, flow cytometric analysis was performed with a FACSCalibur (BD Biosciences).

Magnetic Cell Sorting of AC133$^+$ Cells—Mononuclear cells were labeled with magnetic bead-conjugated anti-AC133 antibodies according to the protocol directed by the manufacturer. After the brief wash with the sorting solution, the cells were separated by a magnetic cell separator (autoMACS, Miltenyi Biotec, Gladbach, Germany), and the positive cells were then collected.

Culture of AC133$^+$ Cells—Isolated AC133$^+$ cells were cultured in EBM-2 (Cambrex Corp., East Rutherford, NJ) medium containing 20% heat-inactivated FBS and 30 mg/liter kanamycin sulfate at 37 °C under moisturized air containing 5% CO_2 with 50 ng/ml VEGF as control medium. Control medium containing VEGF was added with TPO, SCF, or both. Cells were plated on FN- or type IV collagen-coated dishes at a cell density of ~10^6 cells/ml. We have previously shown that EPCs can tightly adhere to an FN-coated dish but weakly to type IV collagen-coated dish (25). Analysis of adherent EPCs was performed on FN-coated dish and that of suspended EPCs on type IV collagen-coated dish. Half of the medium was exchanged once every 3–4 days with fresh medium. Adherent cells on FN-coated dish were fixed with ethanol chilled to −20 °C and then subsequently subjected to an immunostaining procedure or other treatments. Cells on type IV collagen-coated dish were subsequently subjected to flow cytometric analysis.

Immunostaining of Adherent Cells—After fixation with chilled ethanol (−20 °C), the cell layer was washed three times with PBS. Cells were incubated with 1% bovine serum albumin in PBS (−) for 1 h at 4 °C for blocking and then with each first antibody in 1% bovine serum albumin in PBS (−) for 1 h at 4 °C. After washing with PBS, the cells were incubated with FITC-conjugated anti-mouse IgG antibody or rhodamine-conjugated anti-rabbit IgG antibody for 1 h at 4 °C. Cells were washed with PBS and then examined using a Zeiss LSM 510 microscope with an excitation wavelength of 488 nm and an emission of 530/30 nm for FITC or 570/30 nm for rhodamine.

In every experiment, we used nonspecific immunoglobulin corresponding to the first antibody species as a control and confirmed that the cells were not stained with control immunoglobulin. The fluorescence intensity of 20 randomly selected cells was calculated using the Scion Image program within the linear range for quantitation.

Analysis of Cytokines in the Supernatant of CD31^{bright} and CD31$^+$ Cells—The expression of CD31 on cultured AC133$^+$ cells was determined with a flow cytometer. After AC133$^+$ cells were cultured for several days on either FN-coated or collagen type IV-coated dishes, both adherent and nonadherent cells were collected. The collected cells were labeled with FITC-labeled anti-CD31 antibody for 15 min at 4 °C. After a brief wash with 0.5% bovine serum albumin in PBS, flow cytometric analysis was performed. CD31^{bright} and CD31$^+$ cells were sorted from cultured AC133$^+$ cells with FACSAria (BD Biosciences). Sorted cells of both populations were subsequently cultured in EBM-2 supplemented with 20% FBS in the absence of any cytokines. After 5 days, the collected supernatant of cells was frozen at −20 °C. Cytokines were measured by a BD™ cytometric beads array Flex set system (BD Biosciences) according to the manufacturer's protocol.

Flow Cytometric Analysis of Various Cell Surface Markers in Cultured AC133$^+$ Cells—After AC133$^+$ cells were cultured for the indicated period, cells were co-stained with FITC-labeled anti-CD31 antibody and PE-labeled anti-CD14 antibody or PE-labeled VEcad antibody. Cells were also stained with FITC-labeled anti-CD31 antibody, allophycocyanin-labeled anti-CD110 antibody, and PE-labeled anti-AC133 antibody triply and then subjected to flow cytometry. Dead cells were eliminated by staining with 7-amino actinomycin D.

Calculation of the Absolute Number of CD31^{bright} Cells—The absolute number of CD31^{bright} cells was multiplied by the total cell number of each well, and the ratio of CD31^{bright} cells was analyzed by fluorescence-activated cell sorter.

Preparation of Cell Lysates and Immunoblotting—After cell sorting, AC133$^+$ cells were suspended in 20% FBS-EBM2 and cultured for 3 days in the presence of VEGF and TPO. Cells were collected and incubated in 2% FBS-EBM2 for 1 h. Cells were stimulated by 50 ng/ml TPO, 50 ng/ml VEGF, or both for 15 min. Cells (1 × 10^6) were collected and lysed in lysis buffer containing 1% Triton X-100, 10 mM K_2HPO_4/KH_2PO_4 (pH

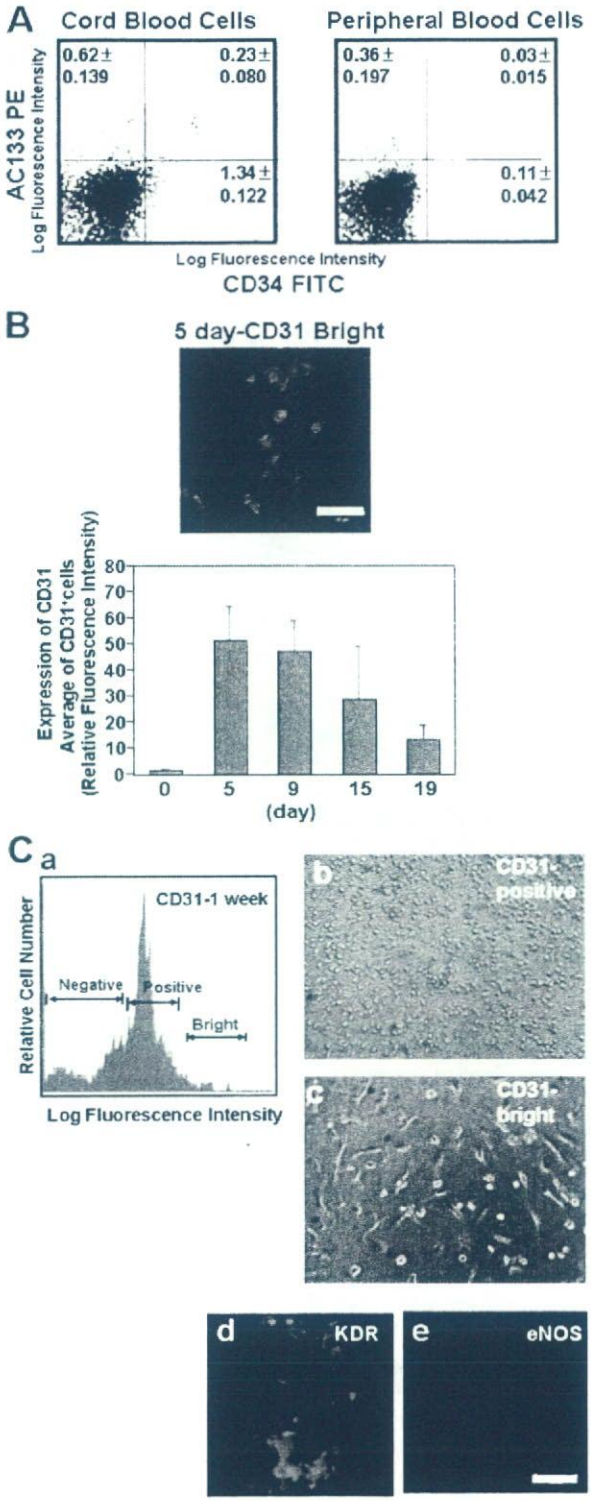

FIGURE 1. ***In vitro* differentiation of AC133$^+$ cells of cord blood into endothelial cells.** *A*, expression of AC133 and CD34 cells in human cord blood and peripheral blood mononuclear cells was analyzed by staining with AC133-PE (*vertical axis*) and CD34-FITC (*horizontal axis*). The *numbers* in the flow cytometric dot blots indicates the percentage of each population ± S.D. *B*, when AC133$^+$ cells were cultured for 19 days in the presence of VEGF on FN-coated dishes, the appearance of CD31$^+$ cells was analyzed. The *upper panel* shows the fluorescent photomicrograph of adhesion cells stained with FITC-conjugated anti-CD31 antibody after a 5-day culture. Quantitation of the fluorescence intensity of 20 CD31-positive cells was analyzed as described under "Experimental Procedures." Columns and bars represent the means ± S.D. from 20 cells (*B*, *lower panel*). *C*, the CD31-negative, positive, and bright cell populations prepared after 1-week cultivation of AC133$^+$ cells are shown in a representative histogram stained with FITC-conjugated anti-CD31 antibody. The *x* axis represents the log fluorescence intensity of CD31-FITC, *y* axis relative cell number (*panel a*). *Panels b* and *c* show phase-contrast microscopic photographs of cultured CD31-positive and bright cells, respectively, subsequently cultured for 1 week after cell sorting. The *bottom panels d* and *e* show the fluorescent photomicrographs of adhesion cells from the CD31^{bright} fraction stained with anti-KDR antibody and anti-eNOS antibody, respectively. *Scale bar*, 100 μm.

7.5), 1 mM EDTA, 5 mM EGTA, 10 mM $MgCl_2$, and 50 mM β-glycerophosphate, along with 1/100 (v/v) protease inhibitor mixture (Sigma) and 1/100 (v/v) phosphatase inhibitor mixture (Sigma). The cellular lysate of 5×10^5 cells/lane was subjected to Western blotting analysis.

Statistical Analysis—Statistical analysis was performed using the unpaired Student's *t* test, and the dose response of TPO was compared between the four groups by one-way analysis of variance and the Tukey test using Prism 4 software. Values of $p < 0.05$ were considered to indicate statistical significance. Each experiment was repeated three times, and the representative data are indicated.

RESULTS

We previously reported that during the *in vitro* differentiation of peripheral blood AC133$^+$ cells into the endothelial cells, the expression of CD31 was the earliest marker among all of the tested markers (25). Moreover, by analyzing the ability of differentiation into endothelial cells, CD31^{bright} cells were shown to exhibit EPC character when compared with the CD31$^+$ fraction. Since cord blood is a rich source of blood stem cells such as CD34$^+$ and AC133$^+$ cells, it is expected to be a useful source for CD31^{bright} cells. At first, we attempted to determine whether the CD31^{bright} fraction derived from cord blood AC133$^+$ cells contained EPCs. As shown in Fig. 1*A*, the populations of AC133$^+$ CD34$^-$ cells, AC133$^-$ CD34$^+$ cells, and AC133$^+$ CD34$^+$ cells in cord blood were approximately four times greater than those in peripheral blood (Fig. 1*A*). After 5 days of cultivation of AC133$^+$ cells on an FN-coated dish, adherent CD31-positive cells were observed (Fig. 1*B*, *upper panel*). Analysis of the fluorescence intensity of CD31-positive cells revealed that the average fluorescence intensity in CD31$^+$ cells was highest on day 5 (Fig. 1*B*, *lower panel*), corresponding to the results of peripheral blood cells.

After 1 week of cultivation of AC133$^+$ cells on a collagen type IV-coated dish, on which cells adhered more loosely when compared with the FN-coated dish, cells were collected and sorted into CD31$^+$ and CD31^{bright} fractions, as shown in Fig. 1*C*, *panel a*, and both cell types were cultured on an FN-coated dish for 1 week after the sorting. The number of cells adhering and spreading was higher in the CD31^{bright} fraction (Fig. 1*C*, *panel c*) than in the CD31$^+$ fraction (Fig. 1*C*, *panel b*), and these adhering cells are apparently KDR- (Fig. 1*C*, *panel d*) and eNOS-positive (Fig. 1*C*, *panel e*). The large areas of intense green fluorescence represent the colonies of CD31^{bright} cells. These data indicate that CD31^{bright} cells derived from AC133$^+$ cells of both peripheral blood and cord blood are EPCs.

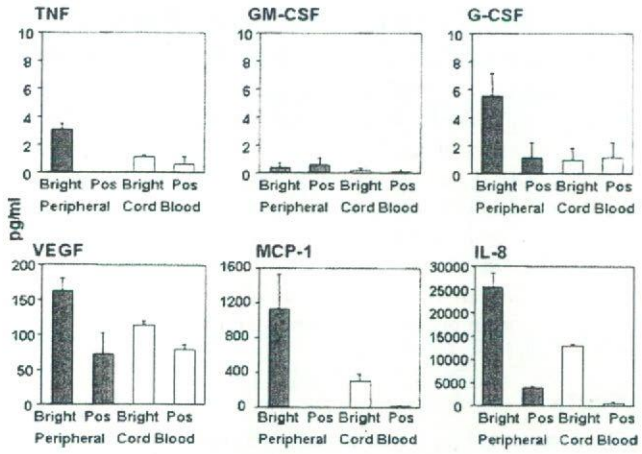

FIGURE 2. **Various cytokines released from CD31$^+$ cells and CD31^{bright} cells.** Production of various cytokines from CD31$^+$ cells and CD31^{bright} cells derived from AC133$^+$ cells cultivated for 5 days was measured. *Gray columns* indicate the cytokine production by cells from peripheral blood and open columns from cord blood. Columns and bars represent the means ± S.D. from three separate experiments. *TNF*, tumor necrosis factor; *Pos*, positive; *MCP-1*, monocyte chemoattractant protein-1.

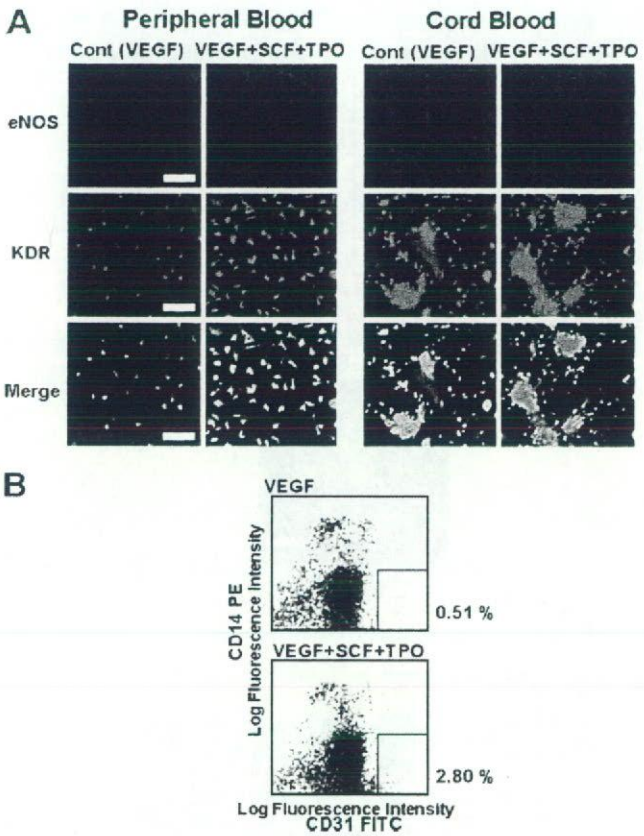

FIGURE 3. **Increment of EPCs from AC133$^+$ cells in the presence of TPO and SCF.** *A*, AC133$^+$ cells were differentiated for 2 weeks in the presence of either VEGF alone or the combination of TPO, SCF, and VEGF on an FN-coated dish. The *upper* and *middle panels* indicate the fluorescent photomicrographs of cells stained with anti-eNOS antibody and anti-KDR antibody, respectively. The *bottom panels* indicate the merged images of both antibodies. From the *left side*, control (*Cont*) and the mixture of peripheral blood, control, and the mixture of cord blood. *Scale bar*, 100 μm. *B*, CD14 and CD31 expression in cultured AC133$^+$ cells for 1 week was stained with CD14-PE (*vertical axis*) and CD31-FITC (*horizontal axis*). The *upper panel* indicates cells treated with VEGF alone, and the *lower panel* indicates cells treated with the mixture of VEGF, SCF, and TPO. The *number* on the *right side* of the flow cytometric dot blot indicates the percentage of the CD14$^-$ CD31^{bright} population.

Several reports have shown that EPCs produce cytokines (9, 26, 27), but the ability of CD31$^+$ or CD31^{bright} cells derived from AC133$^+$ cells to produce cytokines is not known. After cell sorting, quantitative analysis of cytokines released by CD31$^+$ cells and CD31^{bright} cells was carried out at 5 days after the cultivation. As shown in Fig. 2, IL-8 was markedly produced by CD31^{bright} cells from both peripheral blood and cord blood when compared with CD31$^+$ cells. The production of monocyte chemoattractant protein-1 (MCP-1) by CD31^{bright} cells was also higher than that of CD31$^+$ cells. The production of VEGF was higher by CD31^{bright} cells than by CD31$^+$ cells but not significantly. The production of all cytokines by CD31^{bright} cells from peripheral blood was higher than that from cord blood. Tumor necrosis factor-α, GM-CSF, and G-CSF were hardly produced by CD31^{bright} and CD31$^+$ cells. These data indicate that CD31^{bright} cells derived from AC133$^+$ cells have a strong ability to produce chemokines.

It has been reported that TPO and SCF are potent stimulators of multipotent cell proliferation (17, 19). Next, the effects of both growth factors on EPC growth and differentiation in our culture system were determined. After the addition of both TPO and SCF for 2 weeks, the expression of eNOS and KDR in adhered cells was analyzed (Fig. 3*A*). Fig. 3*A* clearly indicates that AC133$^+$ cells from both peripheral blood and cord blood differentiate into eNOS$^+$ and KDR$^+$ cells more efficiently in the presence of the mixture of TPO, SCF, and VEGF than of VEGF alone. Flow cytometric analysis revealed that the ratio of CD31^{bright} CD14$^-$ cells increased in the presence of the mixture of TPO, SCF, and VEGF when AC133$^+$ cells were cultured on collagen type IV-coated dish for 1 week (Fig. 3*B*).

We next examined which growth factor is dominant in the induction and proliferation of CD31^{bright} cells. The total cell number of cultured AC133$^+$ cells from both peripheral blood (Fig. 4*A*, *upper panel*) and cord blood (Fig. 4*A*, *lower panel*) significantly increased in the presence of TPO, SCF, or both growth factors when compared with that of VEGF alone during a 1-week period. As shown in Fig. 4*B*, however, the increment in the ratio of the CD31^{bright} cell population was observed only in the presence of TPO. The absolute number of CD31^{bright} cells, calculated by the total cell number and the ratio of the CD31^{bright} cell population, was markedly increased by TPO (Fig. 4*C*). In contrast, SCF induced the increase in total cell number to the same level as TPO (Fig. 4*A*), but it did not induce the increase in either the ratio of the CD31^{bright} cell population (Fig. 4*B*) or the number of CD31^{bright} cells (Fig. 4*C*). Next, we examined whether TPO and VEGF can synergistically affect the induction of CD31^{bright} cells during a 1-week cultivation. As shown in Fig. 4*D*, although VEGF had no effects on the total cell number (Fig. 4*D*, *panel a*), it increased the ratio of the CD31^{bright} cell population to 1.4-fold higher than that of the control (Fig. 4*D*, *panel b*), resulting in a slight increase in the number of CD31^{bright} cells (Fig. 4*D*, *panel c*). Thrombopoietin alone induced an increase in not only the total cell number (Fig. 4*D*, *panel a*) but also the ratio of the CD31^{bright} cell population (Fig. 4*D*, *panel b*), resulting in an ~24-fold increment of the absolute

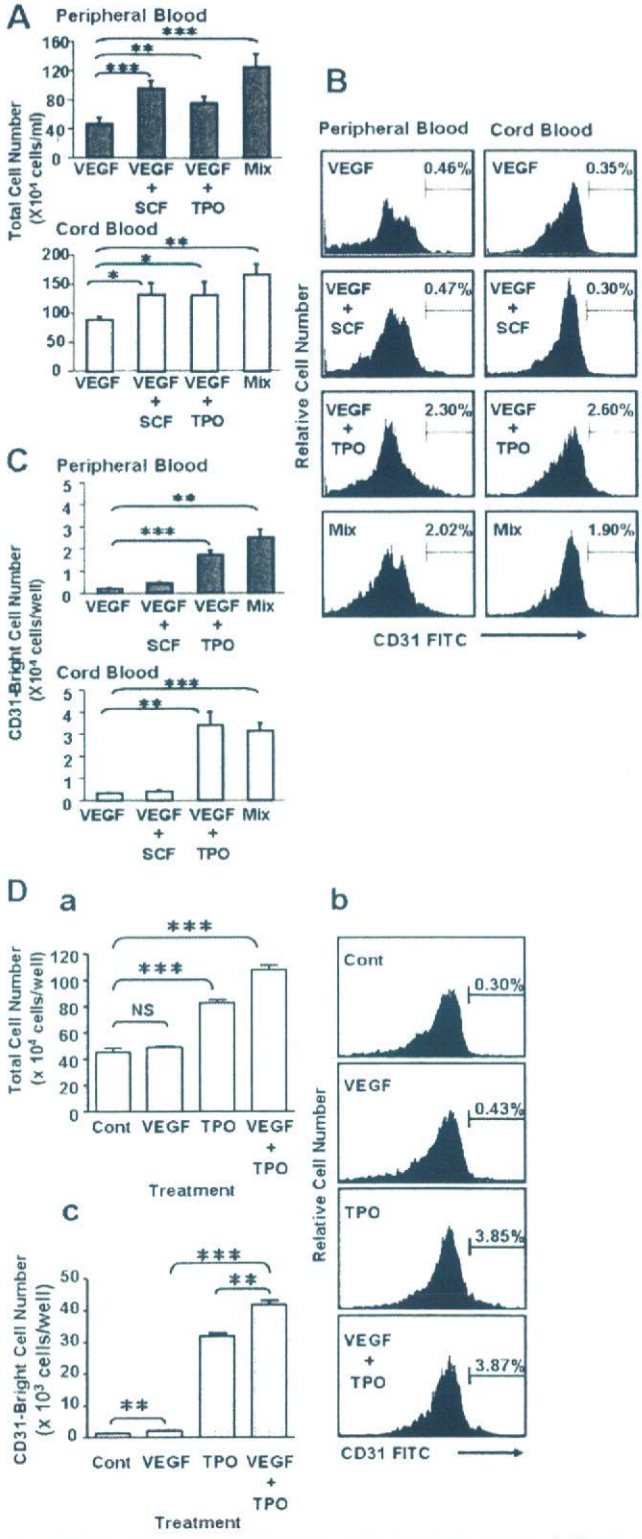

FIGURE 4. **Stimulative effects of TPO on induction of CD31^{bright} cells.** *A*, alteration of the cell number of cultivated AC133$^-$ cells for 1 week in the combination of growth factors. *Mix*, VEGF + SCF + TPO. *B*, the flow cytometric histogram of AC133$^+$-derived cells stained with FITC-labeled anti-CD31 antibody after a 1-week culture. The *representing number* in the flow cytometric histogram indicates the percentage of the CD31^{bright} cell population. The *left panels* are peripheral blood, and the *right panels* are cord blood. *C*, CD31^{bright} cells numbers were calculated by both the total cell number and the ratio the of CD31^{bright} population. *D*, the effects of TPO alone on EPC differentiation derived from AC133$^+$ cells of cord blood. The *upper left panel* (*a*) shows the total cell number after a 1-week culture, the *right panels* (*b*) show the flow cytometric histogram of AC133$^-$-derived cells stained with FITC-labeled anti-CD31 antibody, and the *lower left panel* (*c*) shows the calculated CD31^{bright} cell number. Columns and bars represent the means ± S.D. (*, $p < 0.05$; **, $p < 0.01$; ***, $p < 0.001$). *NS*, not significant; *Cont*, control.

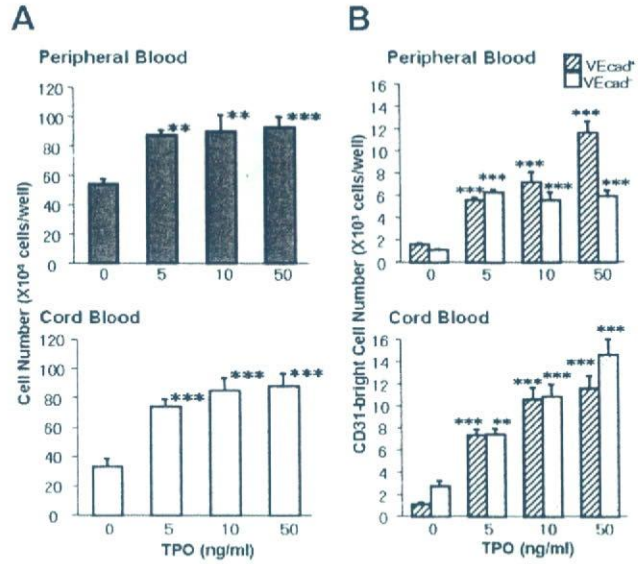

FIGURE 5. **Dose-dependent effects of TPO on the induction of CD31^{bright} cells from AC133$^+$ cells.** AC133$^+$ cells were treated with various concentrations of TPO for 1 week. The *left panels* (*A*) are the total cell number of cultured AC133$^+$ cells from peripheral blood (*upper panel*) and cord blood (*lower panel*). The *right panels* (*B*) are the calculated CD31^{bright} cell number from peripheral blood (*upper panel*) and cord blood (*lower panel*). Columns and bars represent the means ± S.D. (**, $p < 0.01$; ***, $p < 0.001$). *Striped* and *dotted columns* represent CD31^{bright}VEcad$^+$ cells and CD31^{bright}VEcad$^-$ cells, respectively.

number of CD31^{bright} cells when compared with the control (Fig. 4*D*, *panel c*). The concomitant treatment with both VEGF and TPO showed a synergic increase in the number of CD31^{bright} cells (Fig. 4*D*, *panel c*).

When AC133$^+$ cells were cultured with various concentrations of TPO in the presence of constant concentrations of VEGF (50 ng/ml), the total cell number from both peripheral blood (Fig. 5*A*, *upper panel*) and cord blood (Fig. 5*A*, *lower panel*) significantly increased at 5 ng/ml of TPO when compared with the control, and there was no significant difference in the total cell number from 5 to 50 ng/ml of TPO. However, TPO increased the ratio of CD31^{bright} cells of flow cytometry dose-dependently as follows: control, 0.50%; 5 ng/ml, 1.36%; 10 ng, 1.42%; 50 ng/ml 1.90% in peripheral blood and control, 1.16%; 5 ng/ml, 1.99%; 10 ng, 2.51%; 50 ng/ml 2.96% in cord blood. TPO markedly induced the differentiation of AC133$^+$ cells into CD31^{bright}VEcad$^+$ cells in the case of both peripheral blood (Fig. 5*B*, *upper panel*) and cord blood (Fig. 5*B*, *lower panel*) in a dose-dependent manner. In the case of cord blood cells, differentiation into CD31^{bright}VEcad$^-$ cells was also induced by TPO.

The effects of TPO on total cell number during 6-day culture of AC133$^-$ cells were determined. Although the total cell num-

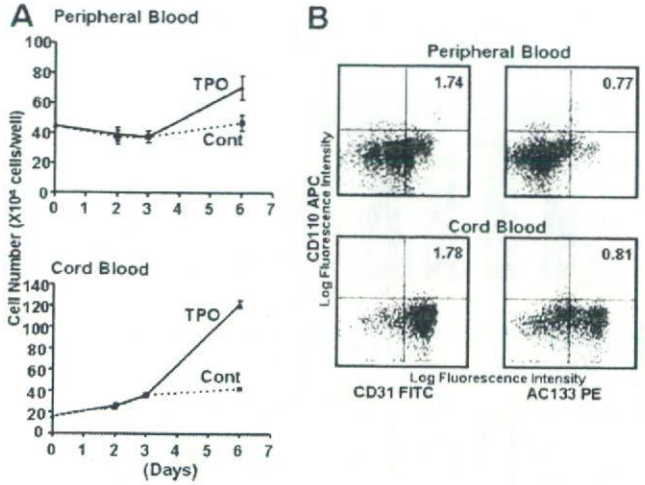

FIGURE 6. **Time-course analysis of TPO-treated AC133$^+$ cells and expression of TPO receptor (CD110).** *A*, alteration of cell number was counted at 2, 3, and 6 days. *Solid* and *dotted lines* indicate TPO-treated cells and control ((*Cont*) VEGF alone) cells, respectively. The results represent mean ± S.E. of triplicate wells. *B*, flow cytometric analysis of CD110 expression on AC133$^+$ cells cultured for 3 days was carried out. The *y axis* represents the log fluorescence intensity of CD110-allophycocyanin (*APC*), and the *x axis* represents that of CD31-FITC (*left panels*) and AC133-PE (*right panels*). The *number* in the flow cytometric dot blot indicates the percentage of CD110$^+$ CD31$^+$ and CD110$^+$ AC133$^+$ populations, respectively. The *upper panels* are peripheral blood, and the *lower panels* are cord blood.

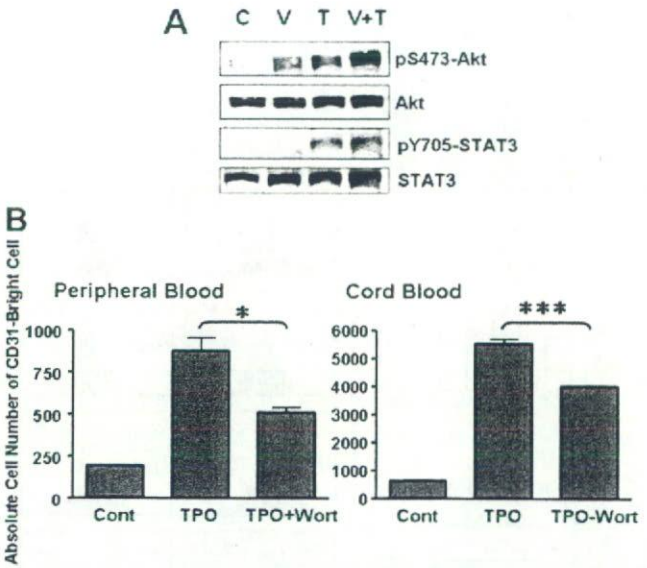

FIGURE 7. **Analysis of TPO-induced signal transduction on AC133$^+$ cells of cord blood.** *A*, activation of Akt or STAT3 was analyzed by Western blotting with anti-phospho-specific Ser-473-Akt antibody (*top panel*) and reprobed with anti-Akt antibody (*second panel*), or with anti-phospho-specific Tyr-705-STAT3 antibody (*third panel*) and reprobed with anti-STAT3 antibody (*lower panel*) after stimulation by VEGF, TPO, or both VEGF and TPO for 15 min using 3-day-cultured AC133$^+$ cells. *C*, control; *V*, VEGF; *T*, TPO. *B*, the effects of wortmannin on CD31^{bright} cell induction were investigated. The *right panel* shows peripheral blood, and the *left panel* shows cord blood. The *y axis* represents the CD31^{bright} cell number. *Wort*, 100 nM wortmannin. Columns and bars represent the means ± S.E. (*, $p < 0.05$; ***, $p < 0.001$). *Cont*, control.

ber from AC133$^+$ cells slightly and constantly increased from day 0 to day 6 in the absence of TPO, total cells markedly increased after the third day in the presence of TPO (Fig. 6*A*). Next, the alternation of TPO receptor (CD110) expression was analyzed during the cultivation of AC133$^+$ cells. Although the percentages of both AC133$^+$ CD110$^+$ cells and CD31$^+$ CD110$^+$ cells were 0% just after magnetic cell sorting, 3 days after the cultivation, ~2% of CD31$^+$ CD110$^+$ cells (Fig. 6*B*, *left panel*) and 1% of AC133$^+$ CD110$^+$ cells (Fig. 6*B*, *right panel*) appeared from AC133$^+$ cells in the peripheral blood and cord blood, respectively. These data indicate the possibility that sorted AC133$^+$ cells may differentiate into AC133$^+$ CD110$^+$ cells and may subsequently proliferate and differentiate into EPCs in response to TPO.

It has been reported that TPO activates the PI3K/Akt pathway (28) or JAK/STAT pathway (20, 29, 30) in target cells. In addition, in the present study, TPO induced a marked proliferation of AC133$^+$ cells after 3-day culture, and CD110 expression in cells cultured for 3 days from both cord blood and peripheral blood was also observed (Fig. 6, *A* and *B*). We then attempted to determine whether TPO activates Akt or STAT in AC133$^+$ cells cultured for 3 days by analyzing the phosphorylation at Ser-473 of Akt or the phosphorylation at Tyr-705 of STAT3, which are the active forms of Akt or STAT3, respectively. As shown in Fig. 7*A*, phosphorylation at Ser-473 of Akt was stimulated by both VEGF and TPO at 15 min and was more markedly stimulated by concomitant treatment with VEGF and TPO than by a single treatment (Fig. 7*A*, *top panel*). Phosphorylation at Tyr-705 of STAT3 was observed only in the presence of TPO, and unlike in the phosphorylation at Ser-473 of Akt, an increased amount of phosphorylation was not observed in the concomitant presence of VEGF and TPO (Fig. 7*A*, *third panel*). On the other hand, there was no difference in the expression of Akt and STAT3 protein levels (Fig. 7*A*, *second panel* and *bottom panel*, respectively). The induction of CD31^{bright} cells was not perfectly but significantly inhibited by wortmannin, an inhibitor of PI3K, suggesting that the PI3K/Akt pathway plays an important role in TPO-induced EPC differentiation (Fig. 7*B*).

DISCUSSION

We have previously reported that CD31^{bright} cells derived from AC133$^+$ cells in human peripheral blood are EPCs (25). In the present study, CD31^{bright} cells also appeared from AC133$^+$ cells prepared from cord blood, which are a rich source of stem cells during the early period of cultivation (Fig. 1, *A* and *B*). When cells were separated in terms of CD31 expression (Fig. 1*C*), CD31^{bright} cells differentiated into KDR-positive and eNOS-positive adherent cells. These data indicate that CD31^{bright} cells derived from AC133$^+$ cells in cord blood have some characteristics similar to those of EPCs in peripheral blood. Although these EPCs in both cord blood and peripheral blood could not form tube-like structure by themselves on Matrigel (data not shown), they secreted angiogenic growth factors (Fig. 2) such as VEGF, IL-8 (31, 32), and monocyte chemoattractant protein-1 (MCP-1) (33). It has been reported that there are at least two types of EPCs: early EPCs and late EPCs. Early EPCs are unable to form tube-like structures and secrete VEGF and IL-8 showing peak growth at 2–3 weeks (9, 26, 27). Late EPCs with the ability to proliferate and having a cobblestone shape appear late at 2–3 weeks, show exponential growth at 4–8 weeks, and have the ability to form tube-like structures

(26, 27, 34). Rehman *et al.* (9) have reported that EPCs derived from monocytes/macrophages do not proliferate but instead release potent proangiogenic growth factors. In many studies (9, 26, 27, 35–37), because the origin of early EPCs was $CD14^+$ cells or was not precluded by monocytic cells, CD14 expression was still observed in the EPCs after cultivation. In our study, in which $AC133^+$ cells were used as the origin of the EPCs, CD14 expression was not observed in $CD31^{bright}$ cells induced by TPO (Fig. 3*B*). Although the $CD31^{bright}$ cells identified as EPCs in this report and in a previous report did not correspond to their cells in terms of the origin of the cells or cell surface markers, these cells may be early EPCs that can release potent proangiogenic growth factors (Fig. 2). In any event, EPCs are thought to be a heterogeneous population, unlike late EPCs, which have a high ability to proliferate.

Circulating EPCs are up-regulated under physiological or pathological conditions and also by 3-hydroxy-3-methyl-glutaryl-CoA reductase inhibitors (14, 15) and cytokines such as erythropoietin (11–13) and G-CSF (10). In this report, we have revealed the possibility of marked expansion of EPCs *in vitro* by TPO. Brizzi *et al.* (20) have reported that TPO directly stimulates endothelial cell motility and neoangiogenesis. In the present study, TPO may have played a stimulatory role in the differentiation of EPCs from circulating stem cells.

Although both TPO and SCF have the same potency with regard to proliferation of $AC133^+$ cells (Fig. 4*A*), TPO specifically induces an increase in the ratio of the $CD31^{bright}$ cell population when compared with SCF (Fig. 4, *B* and *C*). To develop useful cell therapy products for severe ischemia, it has been considered desirable to establish the efficient expansion of EPCs *in vitro*. Thrombopoietin could increase $CD31^{bright}$ cells (EPCs) even in the absence of VEGF. Kirito *et al.* (38) have reported that TPO enhances expression of VEGF in hematopoietic cells through induction of hypoxia-inducible factor 1α. These observations suggest the possibility that the production of EPCs by TPO may be supported by VEGF produced by $AC133^+$ cells. However, from the perspective that TPO and VEGF have synergistic effects on the induction of EPCs, TPO seems to induce EPCs through another signaling cascade.

Thrombopoietin is a major regulator of the proliferation, differentiation, and maturation of megakaryocytes (39, 40). The results from recent studies suggest that TPO can act not only as a lineage-specific hematopoietic growth factor but also can affect other hematopoietic cell types. For example, TPO alone does not induce proliferation of long term repopulating hematopoietic stem cells. However, in combination with SCF or IL-3, TPO has several synergistic effects on cell proliferation (19). Our results have revealed a new role of TPO in the production of EPCs.

In the process of differentiation of $AC133^+$ cells into $CD31^{bright}$ cells, both peripheral blood and cord blood appear to be very similar. $AC133^+$ cells of cord blood, however, have a stronger ability to proliferate than those of peripheral blood (Fig. 6*A*). Moreover, TPO stimulates the induction of $CD31^{bright}VEcad^-$ cells only from cord blood (Fig. 5*B*) at high concentrations. Hur *et al.* (26) have reported that $VEcad^-$ EPCs are thought to be an early EPC. It is therefore thought that $AC133^+$ cells of cord blood are more immature than those of peripheral blood.

Although the total cell number treated with TPO slightly increased in a dose-dependent manner (Fig. 5*A*), the $CD31^{bright}$ cell number markedly increased as the TPO concentration increased (Fig. 5*B*). These data suggest the possibility that a higher concentration of TPO may be needed for $CD31^{bright}$ cell induction from $AC133^+$ cells.

When $AC133^+$ cells were stimulated by TPO or VEGF, an increase in the phosphorylation of Akt at Ser-473 was observed. This increase was strongly enhanced by concomitant treatment with VEGF and TPO (Fig. 7*A*). The induction of $CD31^{bright}$ cells by these growth factors (Fig. 4*D*) was consistent with the increase in the phosphorylation of Akt at Ser-473. TPO but not VEGF could also stimulate the phosphorylation of STAT3 at Tyr-705. We previously reported that the PI3K/p70 S6 kinase pathway and the JAK/STAT3 pathway were important for proliferation and differentiation, respectively, in neutrophilic differentiation (41, 42). Owing to the stimulation of both the PI3K/Akt and the JAK/STAT pathways, we postulated that TPO may be a stronger stimulator of EPC production than VEGF. As shown in Fig. 7*B*, however, wortmannin could not completely inhibit the induction of $CD31^{bright}$ cells. Therefore, a pathway other than the PI3K/Akt pathway may also work for the proliferation and differentiation of EPCs.

The observation of unfavorable angiogenesis has recently been reported after transplantation of bone marrow mononuclear cells in patients with thromboangiitis obliterans (43). Moreover, transfer of both spleen cell-derived EPCs and bone marrow mononuclear cells accelerate atherosclerosis in apoE knockout mice, whereas EPC transfer reduces markers associated with plaque stability (44). These observations suggest that transplantation of differentiated cells from EPCs may be useful therapy as regenerative medicine.

In conclusion, we have demonstrated a new role of TPO in enhancing the differentiation of $AC133^+$ cells into $CD31^{bright}$ cells (EPCs) *in vitro*. These findings may contribute to further development of cell therapy for critical ischemia.

Acknowledgments—We thank Saitama Red Cross of Japan (Saitama, Japan) and Metro Tokyo Red Cross Cord Blood Bank (Tokyo, Japan) for their kind cooperation. We also thank Kirin-Amgen Inc. for their kind gift of recombinant TPO and recombinant SCF.

REFERENCES

1. Asahara, T., Masuda, H., Takahashi, T., Kalka, C., Pastore, C., Silver, M., Kearne, M., Magner, M., and Isner, J. M. (1999) *Circ. Res.* **85,** 221–228
2. Asahara, T., Murohara, T., Sullivan, A., Silver, M., van der Zee, R., Li, T., Witzenbichler, B., Schatteman, G., and Isner, J. M. (1997) *Science* **275,** 964–967
3. Asahara, T., Takahashi, T., Masuda, H., Kalka, C., Chen, D., Iwaguro, H., Inai, Y., Silver, M., and Isner, J. M. (1999) *EMBO J.* **18,** 3964–3972
4. Shi, Q., Rafii, S., Wu, M. H., Wijelath, E. S., Yu, C., Ishida, A., Fujita, Y., Kothari, S., Mohle, R., Sauvage, L. R., Moore, M. A., Storb, R. F., and Hammond, W. P. (1998) *Blood* **92,** 362–367
5. Takahashi, T., Kalka, C., Masuda, H., Chen, D., Silver, M., Kearney, M., Magner, M., Isner, J. M., and Asahara, T. (1999) *Nat. Med.* **5,** 434–438
6. Nieda, M., Nicol, A., Denning-Kendall, P., Sweetenham, J., Bradley, B., and Hows, J. (1997) *Br. J. Haematol.* **98,** 775–777
7. Gill, M., Dias, S., Hattori, K., Rivera, M. L., Hicklin, D., Witte, L., Girardi, L., Yurt, R., Himel, H., and Rafii, S. (2001) *Circ. Res.* **88,** 167–174
8. Peichev, M., Naiyer, A. J., Pereira, D., Zhu, Z., Lane, W. J., Williams, M.,

Oz, M. C., Hicklin, D. J., Witte, L., Moore, M. A., and Rafii, S. (2000) *Blood* **95,** 952–958
9. Rehman, J., Li, J., Orschell, C. M., and March, K. L. (2003) *Circulation* **107,** 1164–1169
10. Kocher, A. A., Schuster, M. D., Szabolcs, M. J., Takuma, S., Burkhoff, D., Wang, J., Homma, S., Edwards, N. M., and Itescu, S. (2001) *Nat. Med.* **7,** 430–436
11. Bahlmann, F. H., De Groot, K., Spandau, J. M., Landry, A. L., Hertel, B., Duckert, T., Boehm, S. M., Menne, J., Haller, H., and Fliser, D. (2004) *Blood* **103,** 921–926
12. Bahlmann, F. H., DeGroot, K., Duckert, T., Niemczyk, E., Bahlmann, E., Boehm, S. M., Haller, H., and Fliser, D. (2003) *Kidney Int.* **64,** 1648–1652
13. Heeschen, C., Aicher, A., Lehmann, R., Fichtlscherer, S., Vasa, M., Urbich, C., Mildner-Rihm, C., Martin, H., Zeiher, A. M., and Dimmeler, S. (2003) *Blood* **102,** 1340–1346
14. Dimmeler, S., Aicher, A., Vasa, M., Mildner-Rihm, C., Adler, K., Tiemann, M., Rutten, H., Fichtlscherer, S., Martin, H., and Zeiher, A. M. (2001) *J. Clin. Investig.* **108,** 391–397
15. Llevadot, J., Murasawa, S., Kureishi, Y., Uchida, S., Masuda, H., Kawamoto, A., Walsh, K., Isner, J. M., and Asahara, T. (2001) *J. Clin. Investig.* **108,** 399–405
16. Kaushansky, K., Lok, S., Holly, R. D., Broudy, V. C., Lin, N., Bailey, M. C., Forstrom, J. W., Buddle, M. M., Oort, P. J., Hagen, F. S., Roth, G. J., Papayannopoulou, T., and Foster, D. C. (1994) *Nature* **369,** 568–571
17. Fox, N., Priestley, G., Papayannopoulou, T., and Kaushansky, K. (2002) *J. Clin. Investig.* **110,** 389–394
18. Kimura, S., Roberts, A. W., Metcalf, D., and Alexander, W. S. (1998) *Proc. Natl. Acad. Sci. U. S. A.* **95,** 1195–1200
19. Sitnicka, E., Lin, N., Priestley, G. V., Fox, N., Broudy, V. C., Wolf, N. S., and Kaushansky, K. (1996) *Blood* **87,** 4998–5005
20. Brizzi, M. F., Battaglia, E., Montrucchio, G., Dentelli, P., Del Sorbo, L., Garbarino, G., Pegoraro, L., and Camussi, G. (1999) *Circ. Res.* **84,** 785–796
21. Kaushansky, K., Lin, N., Grossmann, A., Humes, J., Sprugel, K. H., and Broudy, V. C. (1996) *Exp. Hematol.* **24,** 265–269
22. Broudy, V. C., Lin, N. L., and Kaushansky, K. (1995) *Blood* **85,** 1719–1726
23. Kaushansky, K., Broudy, V. C., Grossmann, A., Humes, J., Lin, N., Ren, H. P., Bailey, M. C., Papayannopoulou, T., Forstrom, J. W., and Sprugel, K. H. (1995) *J. Clin. Investig.* **96,** 1683–1687
24. Kobayashi, M., Laver, J. H., Kato, T., Miyazaki, H., and Ogawa, M. (1995) *Blood* **86,** 2494–2499
25. Kanayasu-Toyoda, T., Yamaguchi, T., Oshizawa, T., and Hayakawa, T. (2003) *J. Cell. Physiol.* **195,** 119–129
26. Hur, J., Yoon, C. H., Kim, H. S., Choi, J. H., Kang, H. J., Hwang, K. K., Oh, B. H., Lee, M. M., and Park, Y. B. (2004) *Arterioscler. Thromb. Vasc. Biol.* **24,** 288–293
27. Yoon, C. H., Hur, J., Park, K. W., Kim, J. H., Lee, C. S., Oh, I. Y., Kim, T. Y., Cho, H. J., Kang, H. J., Chae, I. H., Yang, H. K., Oh, B. H., Park, Y. B., and Kim, H. S. (2005) *Circulation* **112,** 1618–1627
28. Miyakawa, Y., Rojnuckarin, P., Habib, T., and Kaushansky, K. (2001) *J. Biol. Chem.* **276,** 2494–2502
29. Drachman, J. G., Sabath, D. F., Fox, N. E., and Kaushansky, K. (1997) *Blood* **89,** 483–492
30. Kirito, K., Watanabe, T., Sawada, K., Endo, H., Ozawa, K., and Komatsu, N. (2002) *J. Biol. Chem.* **277,** 8329–8337
31. Li, A., Dubey, S., Varney, M. L., Dave, B. J., and Singh, R. K. (2003) *J. Immunol.* **170,** 3369–3376
32. Mizukami, Y., Jo, W. S., Duerr, E. M., Gala, M., Li, J., Zhang, X., Zimmer, M. A., Iliopoulos, O., Zukerberg, L. R., Kohgo, Y., Lynch, M. P., Rueda, B. R., and Chung, D. C. (2005) *Nat. Med.* **11,** 992–997
33. Salcedo, R., Ponce, M. L., Young, H. A., Wasserman, K., Ward, J. M., Kleinman, H. K., Oppenheim, J. J., and Murphy, W. J. (2000) *Blood* **96,** 34–40
34. Lin, Y., Weisdorf, D. J., Solovey, A., and Hebbel, R. P. (2000) *J. Clin. Investig.* **105,** 71–77
35. Assmus, B., Schachinger, V., Teupe, C., Britten, M., Lehmann, R., Dobert, N., Grunwald, F., Aicher, A., Urbich, C., Martin, H., Hoelzer, D., Dimmeler, S., and Zeiher, A. M. (2002) *Circulation* **106,** 3009–3017
36. Kalka, C., Masuda, H., Takahashi, T., Kalka-Moll, W. M., Silver, M., Kearney, M., Li, T., Isner, J. M., and Asahara, T. (2000) *Proc. Natl. Acad. Sci. U. S. A.* **97,** 3422–3427
37. Kawamoto, A., Gwon, H. C., Iwaguro, H., Yamaguchi, J. I., Uchida, S., Masuda, H., Silver, M., Ma, H., Kearney, M., Isner, J. M., and Asahara, T. (2001) *Circulation* **103,** 634–637
38. Kirito, K., Fox, N., Komatsu, N., and Kaushansky, K. (2005) *Blood* **105,** 4258–4263
39. Kelemen, E., Cserhati, I., and Tanos, B. (1958) *Acta Haematol. (Basel)* **20,** 350–355
40. Yamamoto, S. (1957) *Acta Haematol. Jpn.* **20,** 163
41. Kanayasu-Toyoda, T., Yamaguchi, T., Uchida, E., and Hayakawa, T. (1999) *J. Biol. Chem.* **274,** 25471–25480
42. Yamaguchi, T., Mukasa, T., Uchida, E., Kanayasu-Toyoda, T., and Hayakawa, T. (1999) *J. Biol. Chem.* **274,** 15575–15581
43. Miyamoto, K., Nishigami, K., Nagaya, N., Akutsu, K., Chiku, M., Kamei, M., Soma, T., Miyata, S., Higashi, M., Tanaka, R., Nakatani, T., Nonogi, H., and Takeshita, S. (2006) *Circulation* **114,** 2679–2684
44. George, J., Afek, A., Abashidze, A., Shmilovich, H., Deutsch, V., Kopolovich, J., Miller, H., and Keren, G. (2005) *Arterioscler. Thromb. Vasc. Biol.* **25,** 2636–2641

THE JOURNAL OF BIOLOGICAL CHEMISTRY VOL. 282, NO. 32, pp. 23117–23128, August 10, 2007

$G\alpha_{12/13}$-mediated Up-regulation of TRPC6 Negatively Regulates Endothelin-1-induced Cardiac Myofibroblast Formation and Collagen Synthesis through Nuclear Factor of Activated T Cells Activation*[S]

Received for publication, December 22, 2007, and in revised form, May 25, 2007 Published, JBC Papers in Press, May 28, 2007, DOI 10.1074/jbc.M611780200

Motohiro Nishida[‡], Naoya Onohara[‡], Yoji Sato[§], Reiko Suda[‡], Mariko Ogushi[‡], Shihori Tanabe[§], Ryuji Inoue[¶], Yasuo Mori[‖], and Hitoshi Kurose[‡1]

From the [‡]Department of Pharmacology and Toxicology, Graduate School of Pharmaceutical Sciences, Kyushu University, 3-1-1 Maidashi, Higashi-ku, Fukuoka 812-8582, [§]National Institute of Health Sciences, Setagaya, Tokyo 158-8501, the [¶]Department of Physiology, School of Medicine, Fukuoka University, Jonan-ku, Fukuoka 814-0180, and the [‖]Laboratory of Molecular Biology, Department of Synthetic Chemistry and Biological Chemistry, Graduate School of Engineering, Kyoto University, Kyoto 615-8510, Japan

Sustained elevation of $[Ca^{2+}]_i$ has been implicated in many cellular events. We previously reported that α subunits of G_{12} family G proteins ($G\alpha_{12/13}$) participate in sustained Ca^{2+} influx required for the activation of nuclear factor of activated T cells (NFAT), a Ca^{2+}-responsive transcriptional factor, in rat neonatal cardiac fibroblasts. Here, we demonstrate that $G\alpha_{12/13}$-mediated up-regulation of canonical transient receptor potential 6 (TRPC6) channels participates in sustained Ca^{2+} influx and NFAT activation by endothelin (ET)-1 treatment. Expression of constitutively active $G\alpha_{12}$ or $G\alpha_{13}$ increased the expression of TRPC6 proteins and basal Ca^{2+} influx activity. The treatment with ET-1 increased TRPC6 protein levels through $G\alpha_{12/13}$, reactive oxygen species, and c-Jun N-terminal kinase (JNK)-dependent pathways. NFAT is activated by sustained increase in $[Ca^{2+}]_i$ through up-regulated TRPC6. A $G\alpha_{12/13}$-inhibitory polypeptide derived from the regulator of the G-protein signaling domain of p115-Rho guanine nucleotide exchange factor and a JNK inhibitor, SP600125, suppressed the ET-1-induced increase in expression of marker proteins of myofibroblast formation through a $G\alpha_{12/13}$-reactive oxygen species-JNK pathway. The ET-1-induced myofibroblast formation was suppressed by overexpression of TRPC6 and CA NFAT, whereas it was enhanced by TRPC6 small interfering RNAs and cyclosporine A. These results suggest two opposite roles of $G\alpha_{12/13}$ in cardiac fibroblasts. First, $G\alpha_{12/13}$ mediate ET-1-induced myofibroblast formation. Second, $G\alpha_{12/13}$ mediate TRPC6 up-regulation and NFAT activation that negatively regulates ET-1-induced myofibroblast formation. Furthermore, TRPC6 mediates hypertrophic responses in cardiac myocytes but suppresses fibrotic responses in cardiac fibroblasts. Thus, TRPC6 mediates opposite responses in cardiac myocytes and fibroblasts.

Structural remodeling of the heart is a key determinant of clinical outcome in heart disease (1–3). Such remodeling involves the overproduction of ECM[2] proteins, predominantly collagen types I and III, into the interstitial and perivascular space. Excessive collagen deposition increases myocardial stiffness and leads to diastolic dysfunction (2–4). Cardiac fibroblasts, constituting 60–70% of total cell numbers in the heart, are responsible for collagen deposition and create the scaffold for cardiac myocytes. Transformation of cardiac fibroblasts to myofibroblasts, characterized by the expression of α-SMA, has been implicated in diseases with increased ECM deposition and resultant cardiac fibrosis (4–6). Myofibroblast formation is controlled by various profibrotic stimuli, such as growth factors, cytokines, and mechanical stretch (5–8). Although several hormones, such as Ang II and ET-1, that stimulate G protein-coupled receptors also induce myofibroblast formation (9, 10), the molecular mechanism is not fully understood.

Sustained elevation of $[Ca^{2+}]_i$, induced by increased Ca^{2+} influx, is important for the regulation of diverse cellular processes, such as gene expression, cell proliferation, and differentiation.

* This work was supported by grants from the Ministry of Education, Culture, Sports, Science, and Technology of Japan (to M. N. and H. K.); from the Ministry of Health, Labour, and Welfare of Japan and the National Institute of Biomedical Innovation (MF-16) (to Y. S.); from the Program for Promotion of Fundamental Studies in Health Sciences of the National Institute of Biomedical Innovation (NIBIO), the Naito Foundation, and Takeda Science Foundation (to M. N.); and from the Astellas Foundation for Research on Metabolic Disorders and the Kimura Memorial Heart Foundation Research Grant for 2006 (to H. K.). The costs of publication of this article were defrayed in part by the payment of page charges. This article must therefore be hereby marked "*advertisement*" in accordance with 18 U.S.C. Section 1734 solely to indicate this fact.

[S] The on-line version of this article (available at http://www.jbc.org) contains supplemental Figs. 1 and 2.

[1] To whom correspondence should be addressed. Tel./Fax: 81-92-642-6884; E-mail: kurose@phar.kyushu-u.ac.jp.

[2] The abbreviations used are: ECM, extracellular matrix; Ang, angiotensin; CA, constitutively active; CysA, cyclosporine A; DAG, diacylglycerol; DN, dominant negative; DPI, diphenyleneiodonium; EGFR, epidermal growth factor receptor; ET-1, endothelin-1; GFP, green fluorescent protein; JNK, c-Jun NH_2-terminal kinase; NFAT, nuclear factor of activated T cells; p115-RGS, RGS domain of p115Rho guanine nucleotide exchange factor; PLC, phospholipase C; RACC, receptor-activated Ca^{2+} channel; RGS, regulator of G-protein signaling; ROS, reactive oxygen species; RT, reverse transcription; siRNA, small interfering RNA; α-SMA, α-smooth muscle actin; SOCs, store-operated Ca^{2+} channels; TRPC, canonical transient receptor potential; WT, wild type; ERK, extracellular signal-regulated kinase; PP2, 4-amino-5-(4-chlorophenyl)-7-(*t*-butyl)pyrazolo[3,4-*d*]pyrimidine; OAG, a DAG derivative, 1-oleoyl-2-acyl-sn-glycerol.

In the heart, a Ca^{2+}-responsive serine/threonine phosphatase calcineurin is activated by sustained $[Ca^{2+}]_i$ increase, and calcineurin activation has been implicated in hypertrophic growth of cardiomyocytes (11, 12). Activated calcineurin dephosphorylates the transcriptional factor NFAT, facilitating translocation of NFAT from cytosol to the nucleus, where it acts synergistically with other partners to mediate the expression of prohypertrophic genes. However, the physiological and pathological roles of calcineurin-NFAT signaling in cardiac fibroblasts are still controversial when the roles of the signaling pathway are analyzed by CysA, a calcineurin inhibitor. It has been reported that treatment with CysA inhibits pressure overload-induced cardiac hypertrophy and fibrosis (13) and enhances cardiac dysfunction during postinfarction failure (14). Other reports have demonstrated that myocardial fibrosis is promoted in transplanted hearts (15) or chronically aortic banded hearts (16) treated with CysA. Cardiac fibrosis *in vivo* often follows the development of cardiac hypertrophy. To understand fibrotic pathways, it is essential to examine mechanisms of cardiac fibrosis and hypertrophy individually. Although the role of NFAT in cardiac hypertrophy is established, the role of NFAT in cardiac fibrosis is still unknown.

We previously reported that $G\alpha_{12/13}$ mediate Ang II-induced NFAT activation in cardiac fibroblasts (17). We also demonstrated that activation of $G\alpha_{13}$ increases basal Ca^{2+} influx activity, which is completely suppressed by SK&F96365, an inhibitor of RACCs (18). Members of the TRPC family channels are thought to be molecular candidates for RACCs (19). Recent reports have implicated the involvement of TRPC up-regulation in diseases with abnormal Ca^{2+} handling and resultant heart failure (20, 21). We recently reported that TRPC3 and TRPC6 are involved in Ang II-induced hypertrophic responses of rat neonatal cardiomyocytes (12). However, it is still unknown whether TRPC channels participate in $G\alpha_{12/13}$-mediated NFAT activation and agonist-induced myofibroblast formation in cardiac fibroblasts.

In this study, we investigate how the expression of TRPC channels is regulated and whether TRPC channels are involved in the $G\alpha_{12/13}$-mediated increase in basal Ca^{2+} influx required for NFAT activation. We also examine the roles of TRPC channels and NFAT in transformation of cardiac fibroblasts to myofibroblasts.

EXPERIMENTAL PROCEDURES

Materials and Plasmid Construction—JNK inhibitor II (SP600125), cyclosporine A, and PP2 were purchased from Calbiochem. Ang II, ET-1, DPI, U73122, Igepal CA-630, BQ123, BQ788, and anti-α-SMA antibody (clone 1A4) were purchased from Sigma. Fura-2/AM was from Dojindo (Kumamoto, Japan). Collagenase and Fugene 6 were from Roche Applied Science. Dual luciferase reagents was from Promega. pNFAT-Luc and pRL-SV40 vectors were from Stratagene. Anti-TRPC3 and anti-TRPC6 antibodies were from Alomone Laboratories. Anti-TRPC7 antibody was prepared by Y. Mori. Anti-phospho-ERK, anti-ERK, anti-phospho-Src (Tyr^{416}), and anti-Src antibodies were from Cell Signaling. Anti-glyceraldehyde-3-phosphate dehydrogenase, anti-JNK1, horseradish peroxidase-conjugated anti-rabbit IgG, and anti-mouse IgG antibodies were from Santa Cruz Biotechnology, Inc. (Santa Cruz, CA). Anti-Rac antibody was from Transduction Laboratories. CA NFAT was first inserted into the pEGFP-C1 vector (Clontech) and transferred into pShuttle-cytomegalovirus vector to produce recombinant adenovirus. A 913-bp fragment containing the upstream region and the 5′-untranslated region of the rat TRPC6 gene[3] was isolated by PCR using rat genomic DNA as a template, and the fragment was inserted upstream of a luciferase gene in the pGL3-Basic vector using KpnI/BglII sites.

Cell Culture—Cardiac fibroblasts and myocytes were prepared from ventricles of 1–2-day-old Sprague-Dawley rats (17, 22). Briefly, after digestion of ventricles with 0.1% collagenase, isolated fibroblasts were plated on a noncoated dish in Dulbecco's modified Eagle's medium containing 10% fetal bovine serum and 50 units/ml penicillin/streptomycin. Subconfluent cells were serum-starved for 48 h and used for the experiments. Considering the possibility that cardiac fibroblasts may lose the original characteristics after prolonged culture, cells were used within two passages in all experiments.

Production of Adenoviruses, Infection, and Transfection—Recombinant adenoviruses used in this study, including WT TRPC6, DN TRPC6 (C6-3A and C6-ΔN), GFP-fused N-terminal region of NFAT4 (GFP-NFAT4), and CA NFAT, were produced as described previously (12, 23–25). Cells were infected with adenovirus(es) at a multiplicity of infection of 100 for 48 h. Small interference RNAs (100 nM) were transfected with Lipofectamine 2000 for 72 h.

Measurement of Intracellular Ca^{2+} Measurement and NFAT Activity—The intracellular Ca^{2+} concentration ($[Ca^{2+}]_i$) of cardiac fibroblasts was determined by a method described previously (17). Fluorescence images of GFP-positive cells were recorded and analyzed with a video image analysis system (Aquacosmos, Hamamatsu Photonics). Measurement of NFAT activity was performed as described previously (17). For measuring the translocation of GFP-NFAT4, cells (1.5×10^5) plated on glass bottom 35-mm dishes were infected for 48 h with adenovirus coding GFP-NFAT4 at a multiplicity of infection of 30. After ET-1 stimulation (100 nM) for 48 h, the localization of GFP-NFAT4 was determined with a laser-scanning confocal imaging system (LSM510; Carl Zeiss).

Measurement of ROS Production—Measurement of intracellular ROS concentration was performed in 2 mM Ca^{2+}-containing Hepes-buffered saline solution (107 mM NaCl, 6 mM KCl, 11.5 mM glucose, 20 mM HEPES, pH 7.4, 1.2 mM $MgSO_4$, 2 mM $CaCl_2$) with a fluorescent dye, 2′,7′-dichlorofluorescein diacetate as described previously (17). Fluorescence images were recorded and analyzed with a video image analysis system (Aquacosmos, Hamamatsu Photonics). The peak changes ($\Delta F/F_0$) of DCF fluorescence intensity were identified as values obtained by subtracting the basal fluorescence intensity (F_0) from the maximal intensity during 5-min ET-1 treatment.

Expression Analysis of TRPC mRNAs—The RT-PCR protocol used for the expression analysis and the PCR primers used in this study were as described previously (26). Real time RT-PCR for quantitative measurement was performed as described pre-

[3] The sequence was obtained from Ref. 37 (GenBank™ accession number NW_047798).